Development of Design Practices for Additively Manufactured Micro-Mix Hydrogen Fueled Turbine Combustors with High-Fidelity Simulation Analysis, Reduced Modeling and Testing

Gustaaf Jacobs (Professor), Pavel Popov (Assistant Professor), Priyank Dhyani (PhD), Kaku Eduku (PhD), Thomas Keesom (M.S.), Greg Thomson (Consulting Computer Scientist)

San Diego State University

Michael Ramotowski, Yonduck Sung, Raj Patel, Daniel Ryan

Solar Turbines

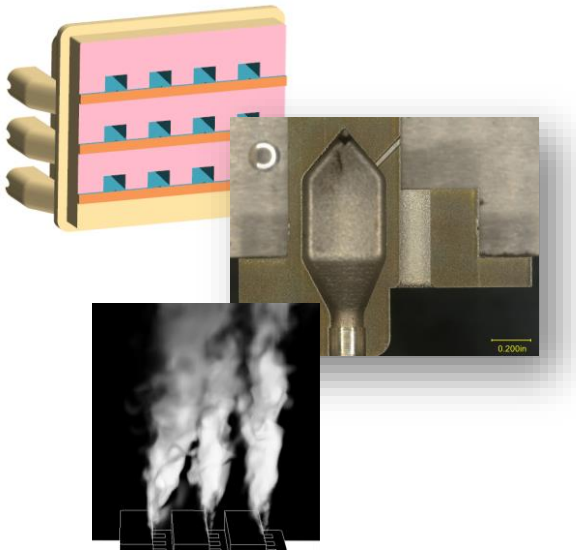

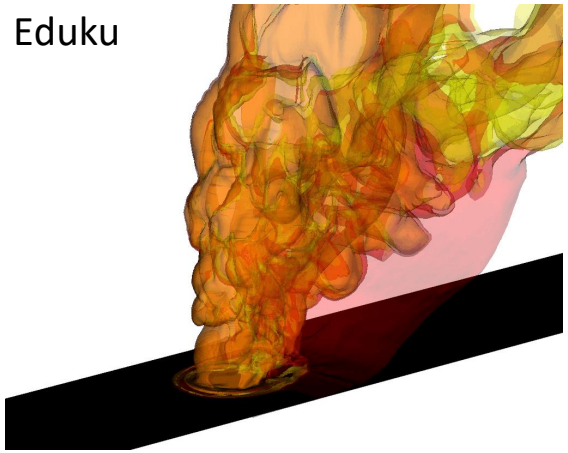

(DE-FOA-0002397)

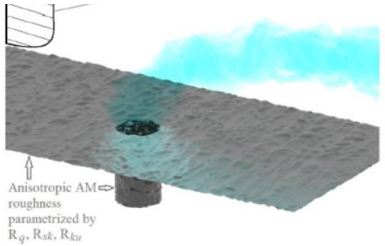

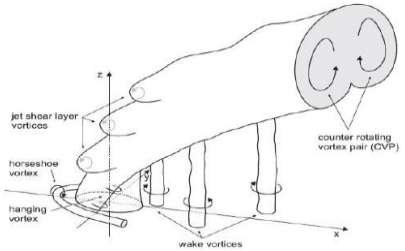

Micro Mixers Considerations

- Conceptually, advantage of micro-mixing include
  - Optimal positioning of the ignition plugs
  - Miniaturization decreases reactant residence times in small reaction zones which significantly reduces NO_x

- Challenges
  - Hydrogen reaction flow physics in micro-mixer environment is unexplored
  - Geometry and flow design are not conducted with fundamental design rules
  - Open questions related to geometry design, optimal flow conditions, predictive models etc…

- Can we manufacture new designs with additive manufacturing techniques?

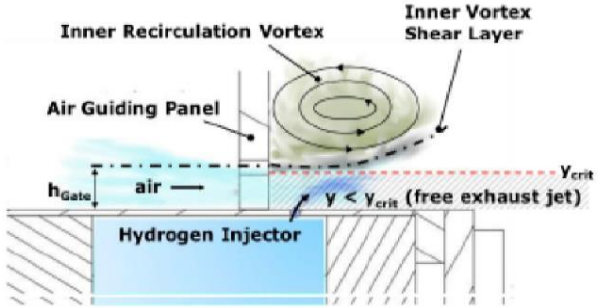

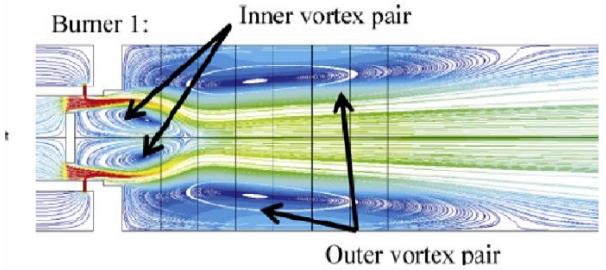

Goals and Approach

1. Determination of foundational design rules for hydrogen micromixer injectors in industrial gas turbine combustors using high-fidelity analysis and testing

   ✓ **Using an established Finite Difference solver to develop and validate a Discontinuous Galerkin solver**

   ✓ **Establish a baseline and generate data**

   1. Chemically reacting flow

2. Development of design tools through reduced models that predict flow mixing, pressure losses, heat transfer and flame stability as a function of geometric and flow design parameters in a computationally efficient manner

2. Assessment of the impact of additive manufacturing on the roughness topography including its anistropy in and around injectors on cold flow and combustion characteristics

Finite Difference Solver with Overset Grid

- Divide computational in overlapping multi-block
- Each block use a 4th order center compact FD scheme
- Interpolate the solution between blocks

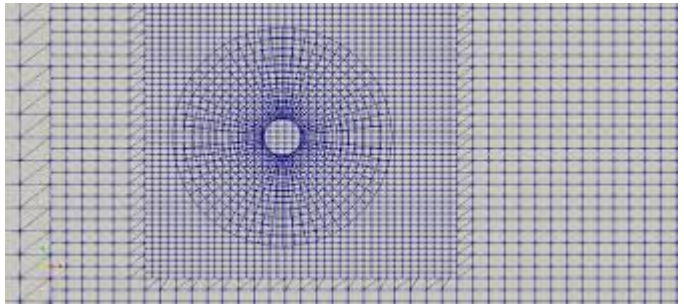

Existing software suite co-developed by Dr. H. Wang, Dr. P. P. Popov, Dr. S. B. Pope

- Advantages:
  - Thoroughly tested for LES with FDMF models
  - Structures grid within blocks provide smooth solutions

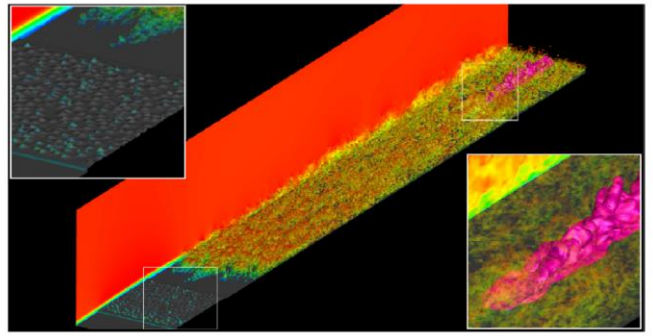

- Downsides:
  - Overset is difficult for complex geometries
  - Overset reduces parallel efficiency
  - FD schemes have overlap at the boundary=> complex boundaries is difficult to handle or loss of accuracy

[Wang, Popov and Pope, JCP, 2010, Popov and Pope, CNF 2014, Popov et al., CNF 2019]

LES with Discontinuous Galerkin Spectral Element Method

- Divide computational domain into elements
- Map each physical element onto a master element
- Approximate solution with higher-order (Jacobi) polynomial

$$f(x_i) \approx \sum_{j=0}^{N} \hat{f}_j L_j(x_i) = \sum_{j=0}^{N} f_j \ell_j(x_i) \qquad f'(x_i) \approx \sum_{j=0}^{N} f_j \ell'_j(x_i)$$

- Based on Method of Weighted Residuals
- Elements are connected through Riemann solvers

✓ Chemically reaction modules are integrated

✓ Basic test verify code

➢ Work has started on wall roughness algorithms

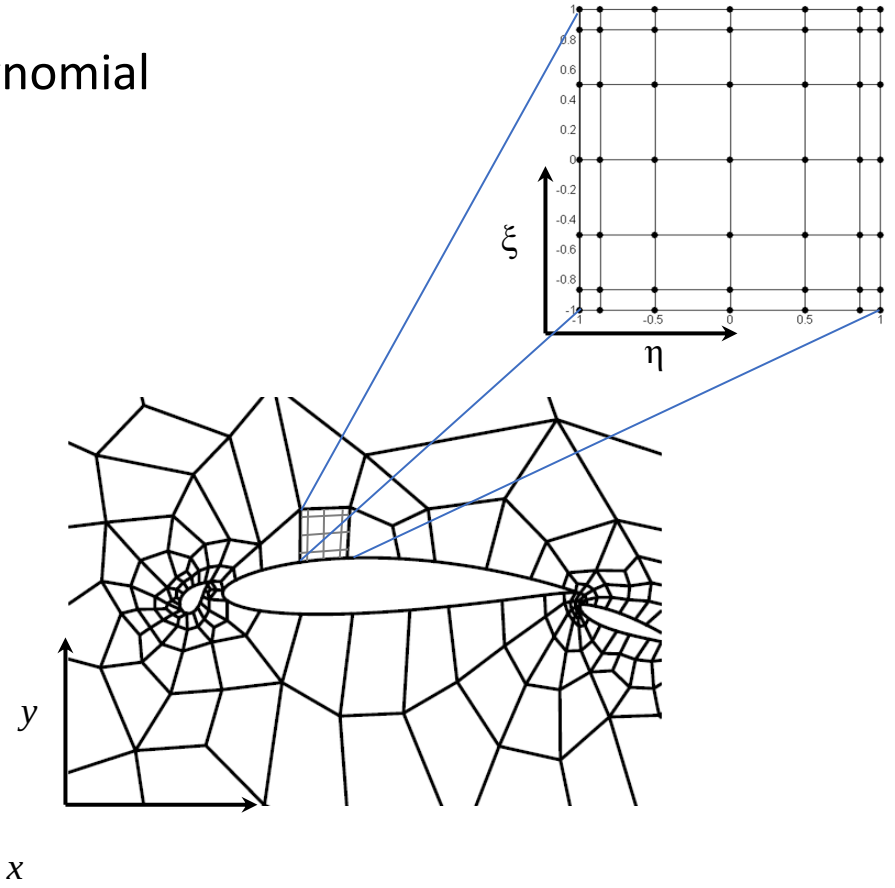

[Jacobs, Kopriva, Mashayek, AIAA J. '06, Chaudhuri, Jacobs, Mashayek, JPC, 2016, Natarajan, Popov, Jacobs, CMAME, 2021]

Semi-Lagrangian DG-FMDF

- Solve the FMDF equation

$$\frac{\partial F_L}{\partial t}+\frac{\partial\left[\widetilde{u}_i F_L-\Gamma_t\frac{\partial(F_L/\langle\rho\rangle)}{\partial x_i}\right]}{\partial x_i}=\frac{\partial}{\partial x_i}\left[\Gamma\frac{\partial(F_L/\langle\rho\rangle)}{\partial x_i}\right]+\frac{\partial}{\partial\psi_\alpha}\left[\Omega(\psi_\alpha-\widetilde{\phi_\alpha})F_L\right]-\frac{\partial[R_\alpha F_L]}{\partial\psi_\alpha}$$

via the equivalent system of equations with ϕ_α species, R_α reaction rates, D is diffusion coefficient

$$d\boldsymbol{X}=\boldsymbol{u}(\boldsymbol{X},t)dt+\sqrt{2D}\,d\boldsymbol{W} \qquad \frac{d\phi_\alpha}{dt}=R_\alpha+\Omega(\widetilde{\phi_\alpha}-\phi_\alpha)$$

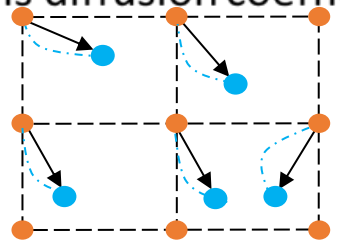

in a semi-Lagrangian manner.

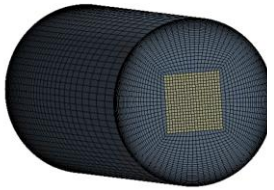

- Advantages for hydrogen micro-mixer simulation include complex geo local, parallel, semi-fixed grid, near-wall accuracy, provably conservative and stable with cfl >1, prevents low particle number density areas

[Natarajan andJacobs, C&F, ’21; Natarajan, Jacobs and Popov, CMAME, ’22]

SL-DG performance: Shear Layer

- $Re = 500, Ma = 0.3, Da \approx 1$
- 9 −species, 12-reaction skeletal $O - H$ chemical mechanism

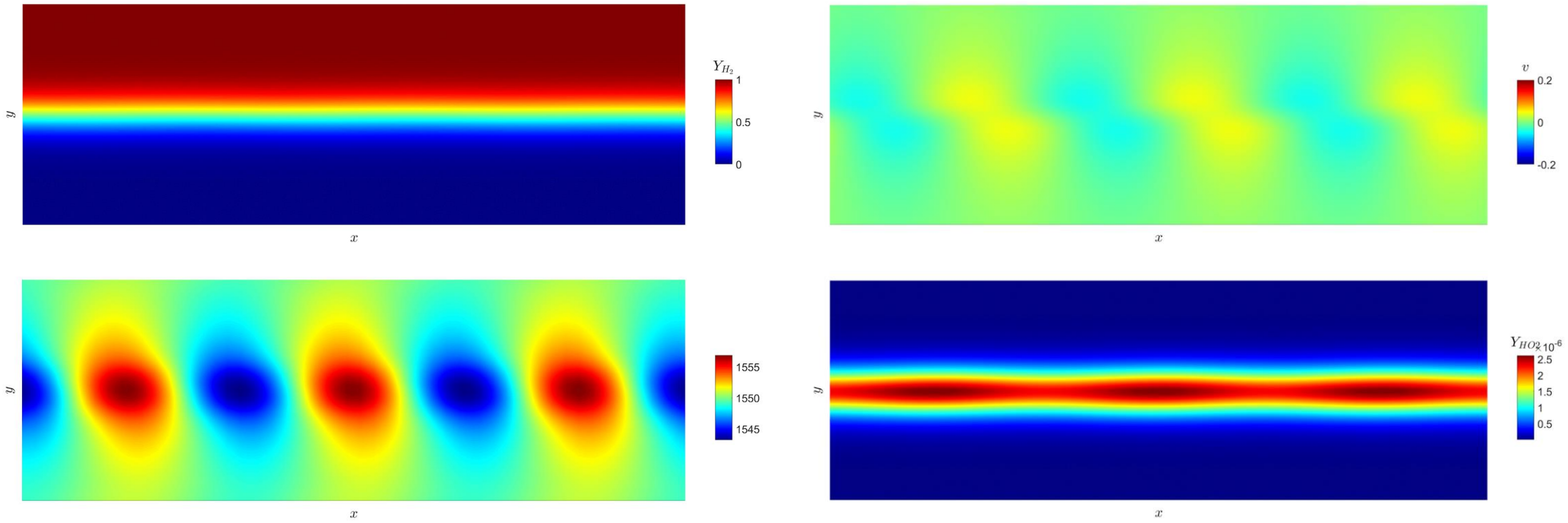

- Heat release is insignificant at first, during radical buildup stage
- Temperature rises rapidly after the initial stage

Implementation of Data-Driven Wall-Roughness Models into DGSEM code

DGSEM for rough walls

- Complex geometries: unstructured grids
- Accurate wall modeling: boundary fitted elements to accurately model roughness element
  - no weird oscillation or reduced accuracy near the wall
- How can we transplant the wall roughness image form material scientists to a CFD code?

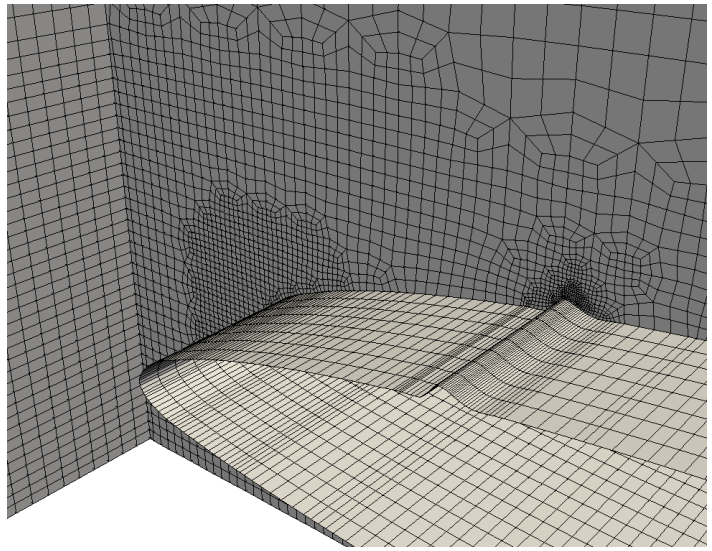

9

From Data to Models for CFD

Challenges

1. Limited data availability: only for small patches are electron-microscope images available
2. CFD meshes and polynomial approximations in CFD codes need a certain smoothness
3. The noisy smaller scale in the roughness images require a grid resolution that is not feasible

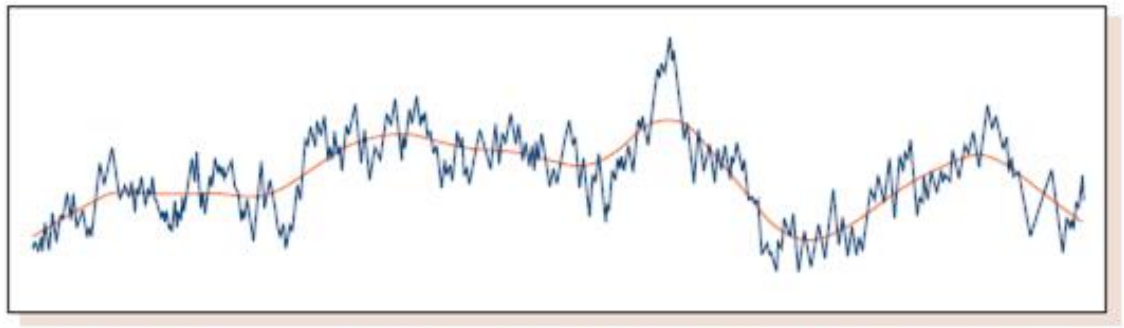

Figure 1: The primary profile and mean line for the primary profile (λ_s cut-off) filter

Can we model the roughness elements with a smooth function that represents the major spatial modes?

Can we extrapolate this information to generate a synthetic wall roughness input for CFD?

Data-Driven Roughness Model

Scanned image of roughness heights

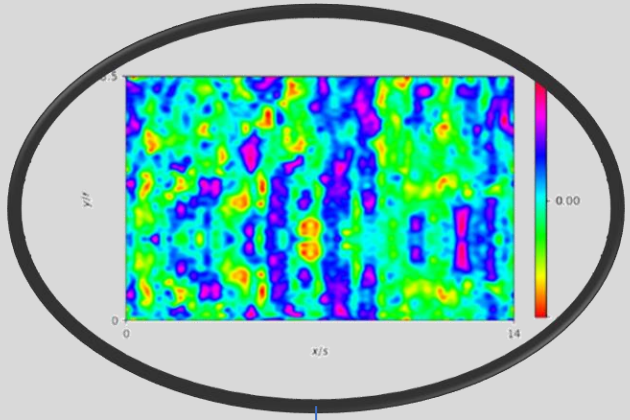

Fit to Fourier Series

$$f^F(x,y) = \sum_{n=-N/2}^{N/2} \sum_{m=-M/2}^{M/2} \hat{f}^F_{nm}(k_n,k_m) e^{k_n x i} e^{-k_m y i}$$

Determine spectra and correlations

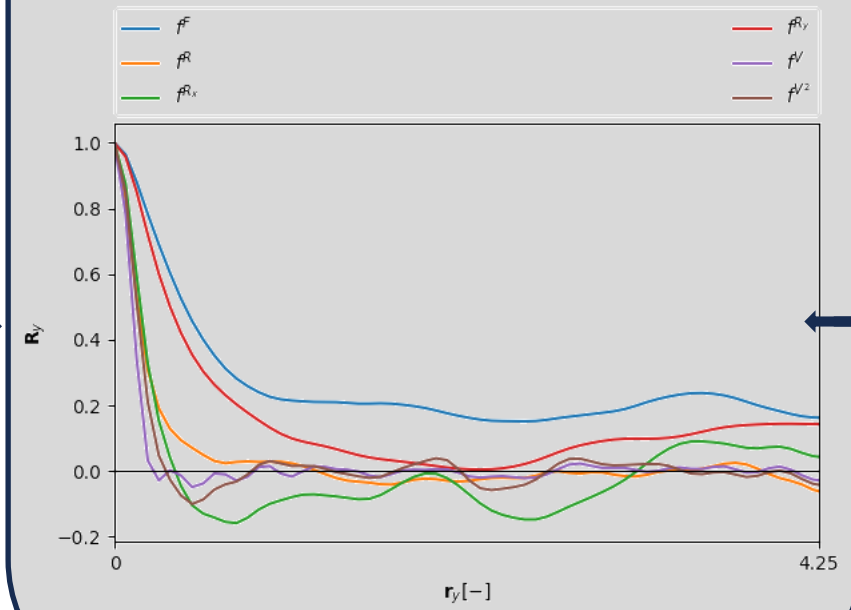

Generate correlated "smooth" roughness fields

$$f^R_y(x,y) = \sum_{n=-N/2}^{N/2} \sum_{m=-M/2}^{M/2} \hat{f}^R_m e^{k_n x i} e^{k_m y i}$$

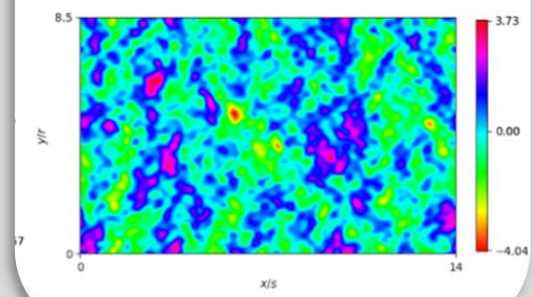

How to translate to CFD code?

DG with Complex Geometries

- The solution is mapped from physical space to the reference element:

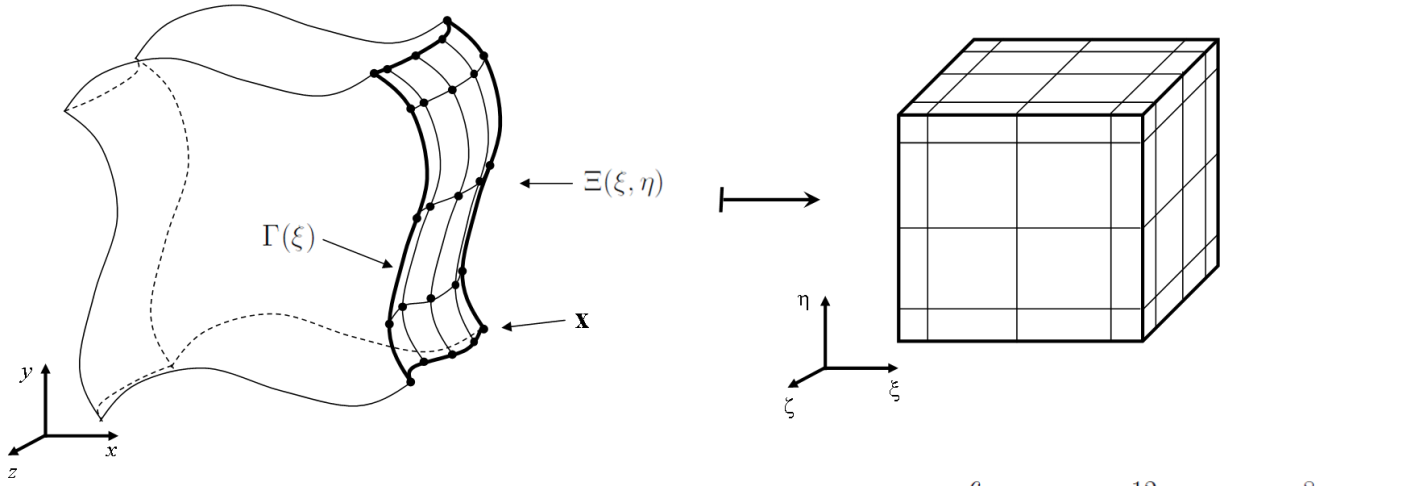

- Mapping incorporates contributions from the faces, edges and corners:

Faces: $$\Xi(\xi,\eta) = \sum_{i=0}^{N}\sum_{j=0}^{N} \mathbf{x}_{ij}\ell_i(\xi)\ell_j(\eta)$$

Edges: $$\Gamma(\xi) = \sum_{i=0}^{N} \mathbf{x}_i \ell_i(\xi)$$

$$\mathbf{x}(\xi,\eta,\zeta) = \sum_{i=1}^{6} p_i\Xi_i + \sum_{i=1}^{12} q_i\Gamma_i + \sum_{i=1}^{8} r_i\mathbf{x}_i$$

p_i, q_i and r_i are shape functions:

e.g. $$r_1 = (1-\xi)(1-\eta)(1-\zeta)$$

- Metric terms and derivatives are computed from the mapping

$$\nabla_{\mathbf{x}} F(\mathbf{x}) = \frac{1}{J}\sum_{i=1}^{3}\frac{\partial}{\partial\xi^i}[(\mathbf{a}_j \times \mathbf{a}_k)F] \quad \text{where} \quad \mathbf{a}_i = \partial\mathbf{x}/\partial\xi_i$$

Compatibility with Grid Software

- Computer-Aided Design (CAD) tools define geometries with non-analytic or piecewise-analytic functions:
  - Splines
  - NURBS
- Grid generation software does not align elements with spline nodes in order to provide more flexibility with mesh refinement
- Grid generation software typically does not produce curved-sided elements

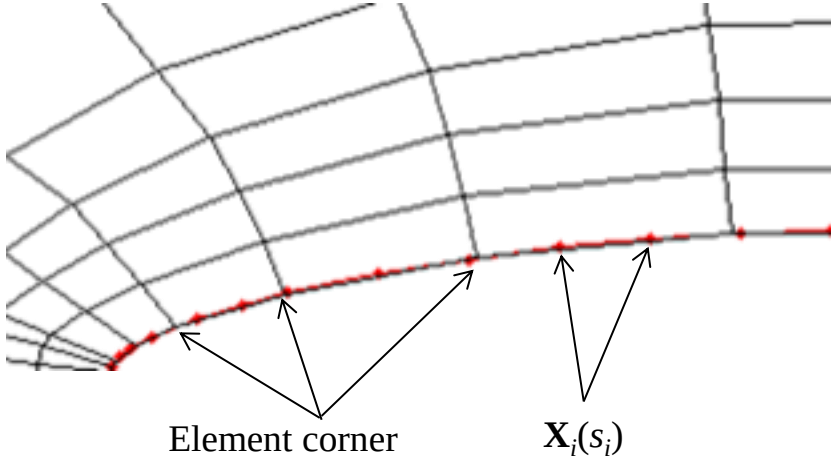

Spline with nodes $\mathbf{X}_i(s_i)$, where s_i is defined by:

$$s'_i = \sum_{j=1}^{i-1} \sqrt{(X_{j+1} - X_j)^2 + (Y_{j+1} - Y_j)^2}$$

and normalized:

$$s_i = \frac{s'_i - s'_1}{s'_n - s'_1}$$

then $\mathbf{X}(s)$ is

$$\mathbf{X}(s) = \mathbf{a} + \mathbf{b}s + \mathbf{c}s^2 + \mathbf{d}s^3$$

Curved-Boundary Meshing

- DG element edges are fit to boundaries defined by splines
  - in two-dimensions:

$$\Gamma(\xi) = \sum_{j=0}^{N} \mathbf{X}(s_j)\ell_j(\xi)$$

$$s_j = \xi_j(s_b - s_a) + s_a$$

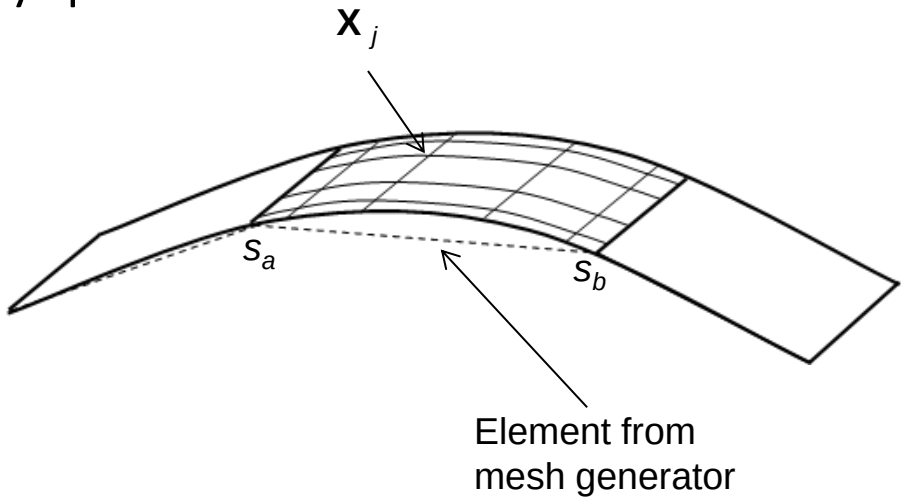

- Higher derivatives are discontinuous in splines
  - We must be careful with high-order approximation of splines

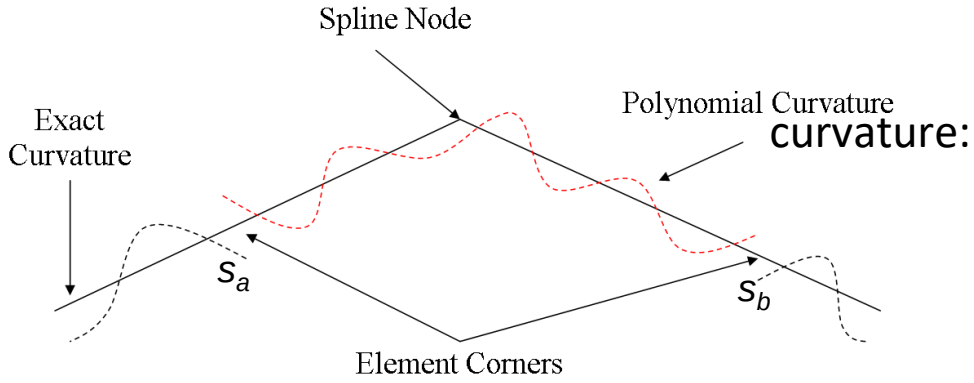

curvature:

$$\kappa(s) = \frac{\left|X'(s)Y''(s) - Y'(s)X''(s)\right|}{\left(\left[X'(s)\right]^2 + \left[Y'(s)\right]^2\right)^{3/2}}$$

Curved Meshes

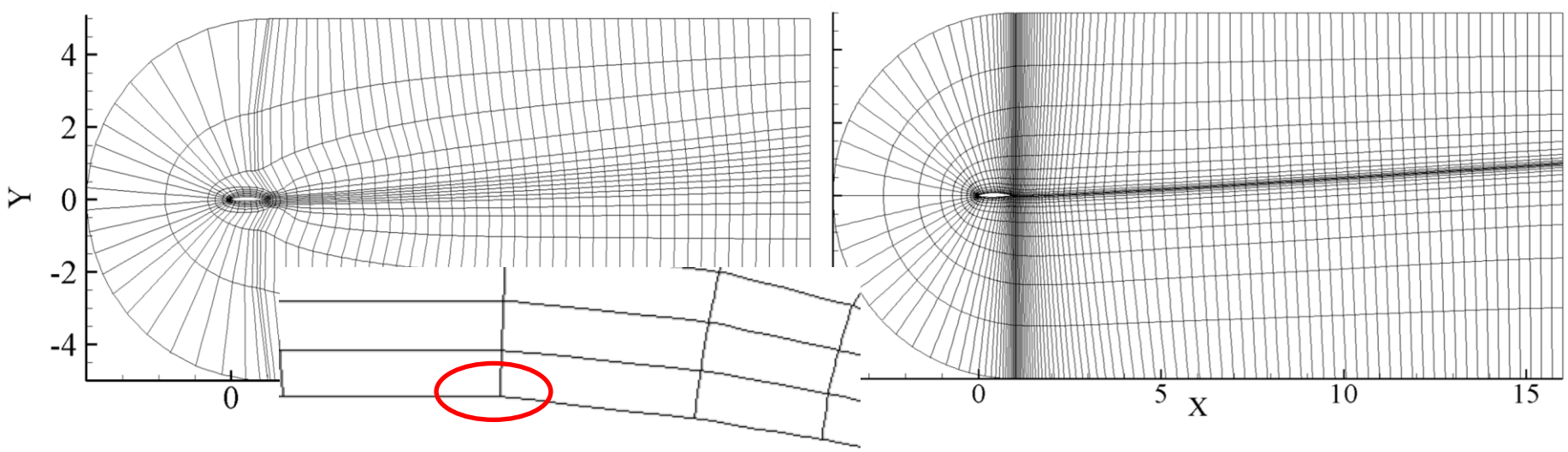

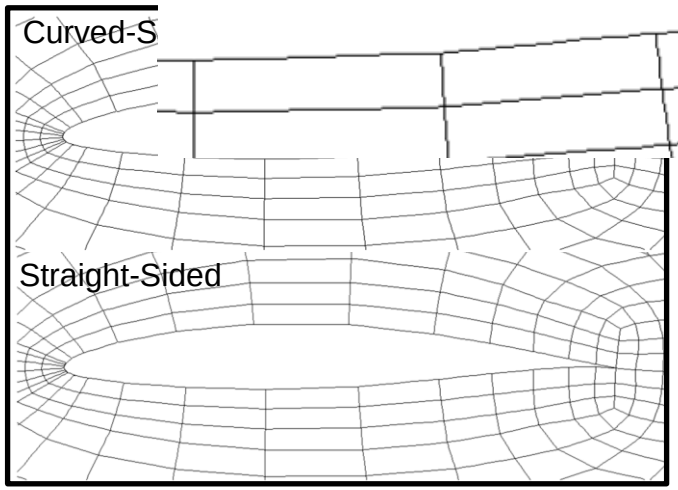

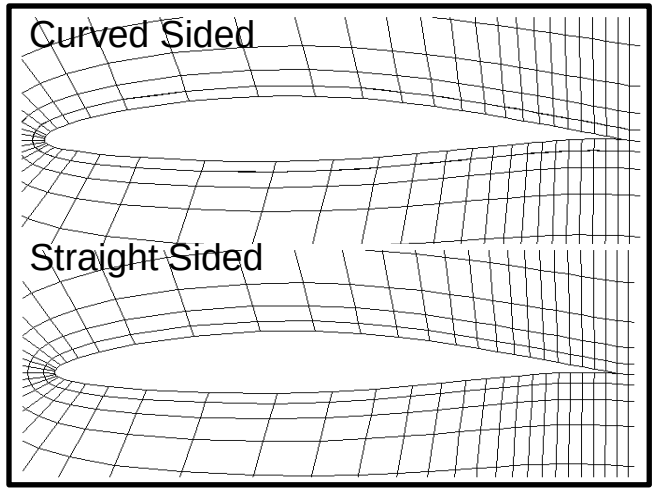

Flow Field

Solution for P = 12 (thirteenth order convergence rate!

Vorticity

Curved-Sided

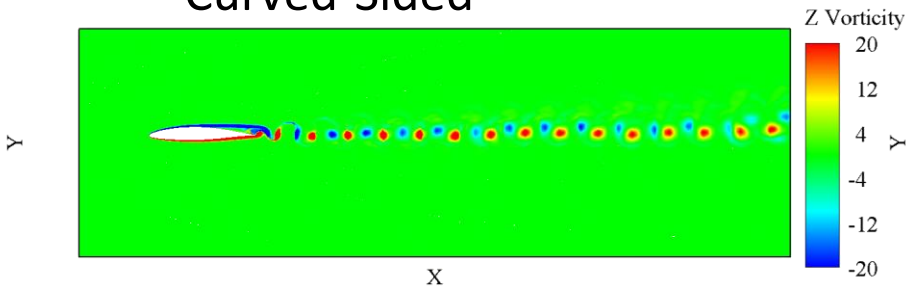

Straight-Sided

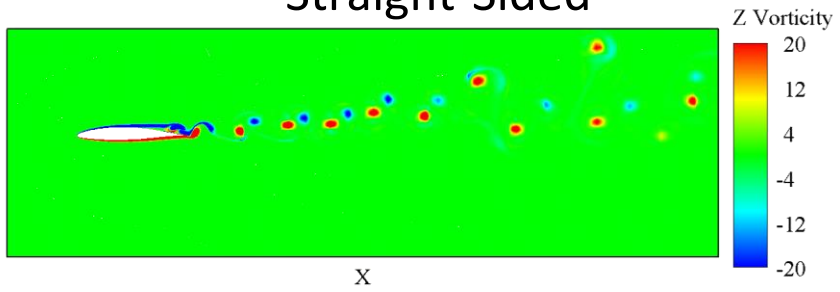

RMS-Velocity

Curved-Sided

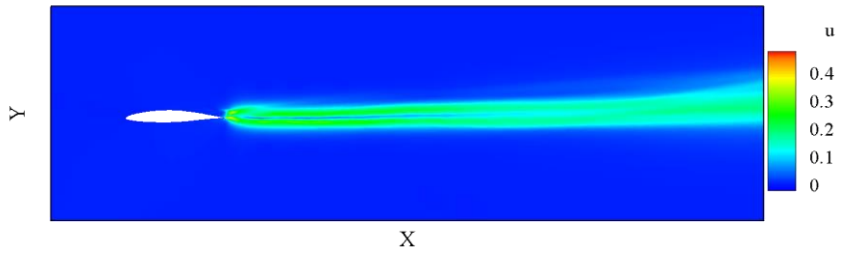

Straight-Sided

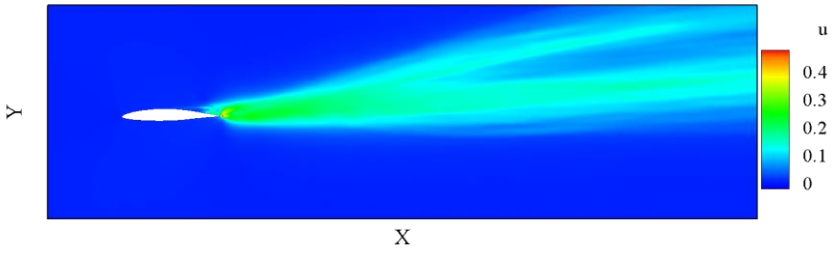

Wall Roughness Investigation

Domain

Wall Boundary fitted to Fourier modes

Grid

Fifth order urved elements

Powerlaw element distribution in wall normal direction

Boundary Conditions

Periodic boundary conditions in x and z-direction

Isothermal walls and free-slip on the top boundary

Initial Condition

Blasius boundary layer

Re=500, Ma=0.3

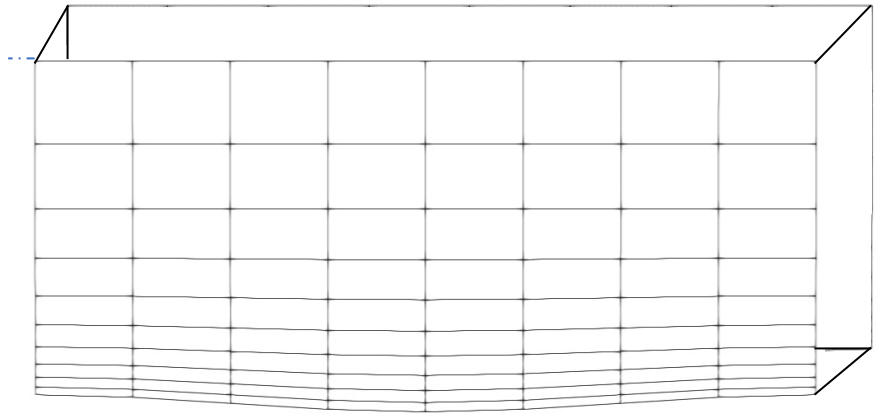

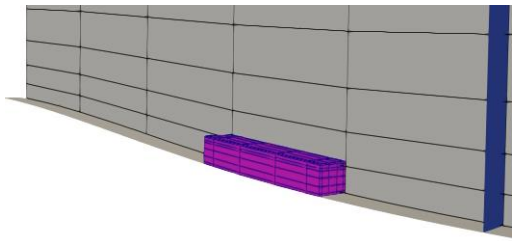

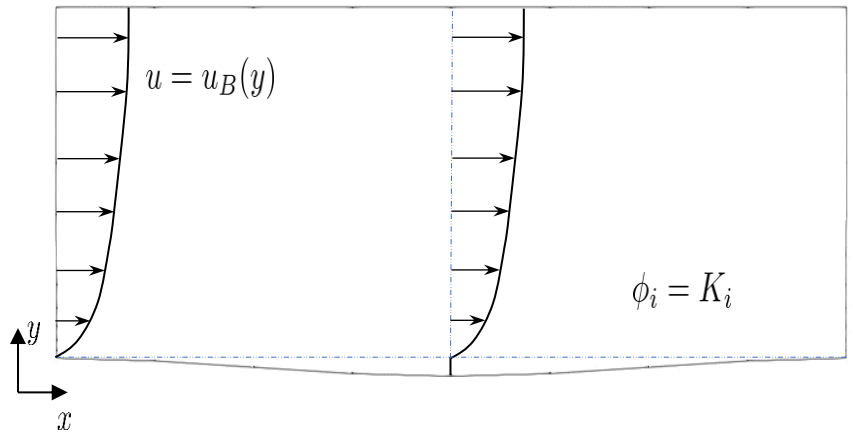

3D Wall Roughness

Flat Wall

$y = 0$

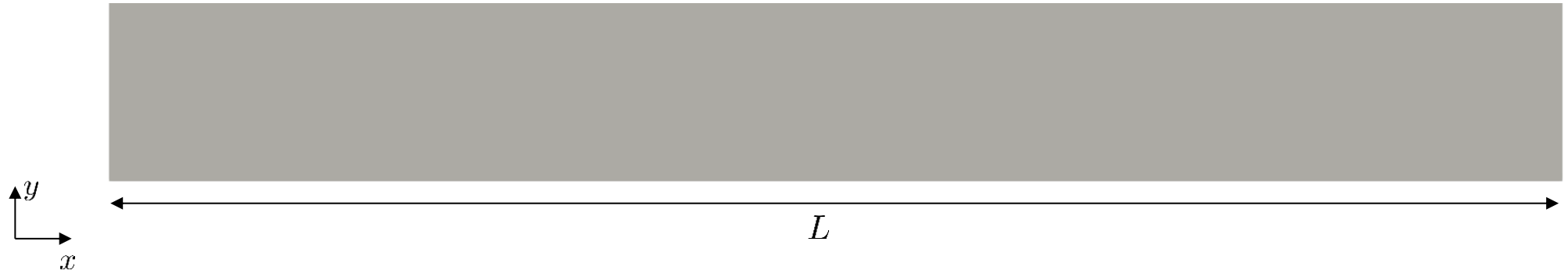

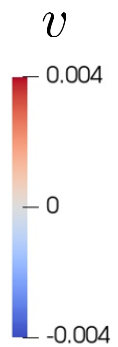

Curved Wall : Single mode

$y = A_1 \cos\left(\frac{2\pi x k_1}{L}\right)$

Curved Wall : Secondary mode

$y = A_1 \cos\left(\frac{2\pi x k_1}{L}\right) + A_2 \cos\left(\frac{2\pi x k_2}{L}\right)$

$A_1 = 0.3; A_2 = 0.06; K_1 = 1; K_2 = 4$

Reacting flow

- The wall temperature ignites the mixture which the the formation of H radicals
- The flame then propgates normal to the wall

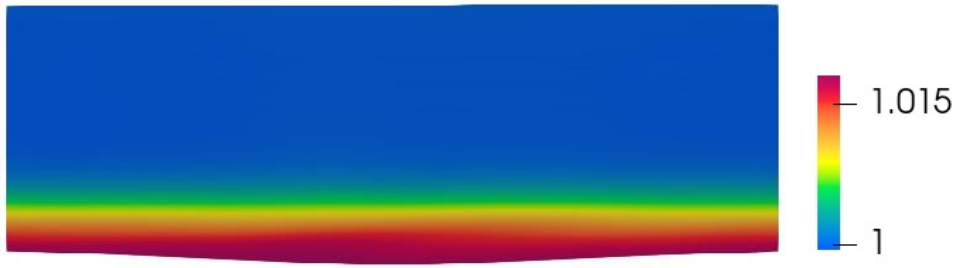

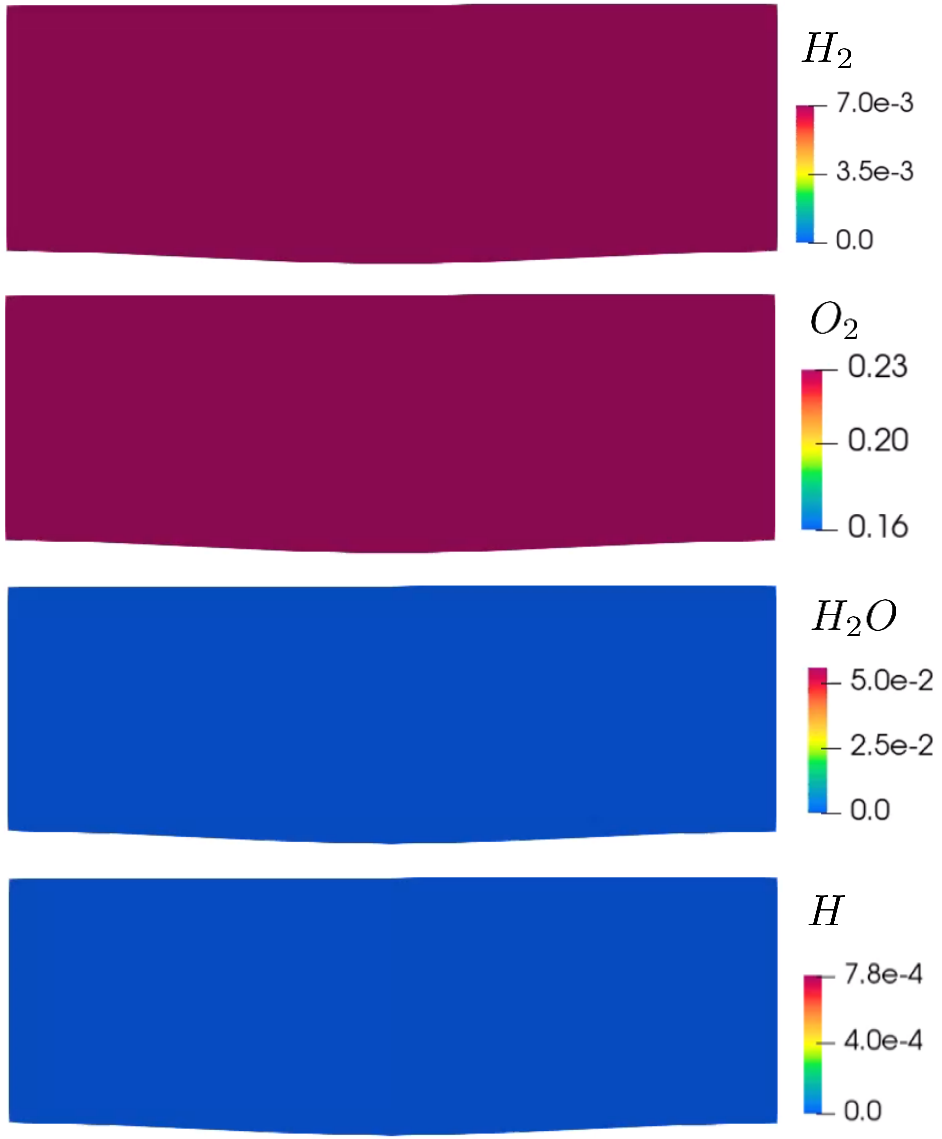

Design Rules Hydrogen Micro-Mixer Simulations: Simulations and Inference of Reduced Models

Solar Turbines - High H2 Combustion Data

- "Micromixer" type fuel injection system for high H2 flames
  - Jet in crossflow configuration for short flames to achieve lower NOx emission
- Test rigs
  - Single and multi-nozzle configurations
  - Elevated temperature up to 800F
  - Various NG-H2 fuel mixtures up to 100% H2

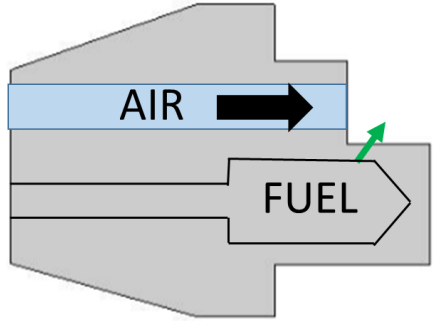

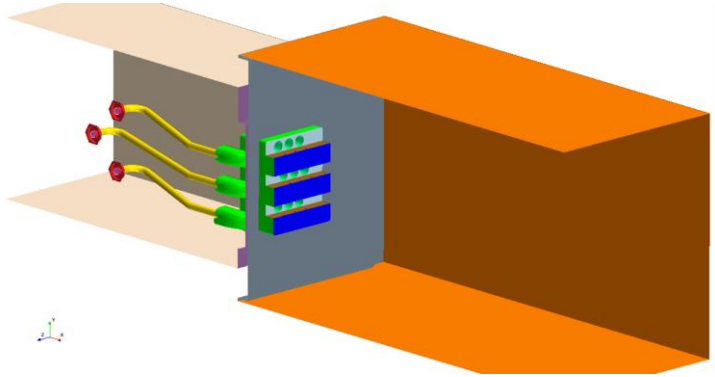

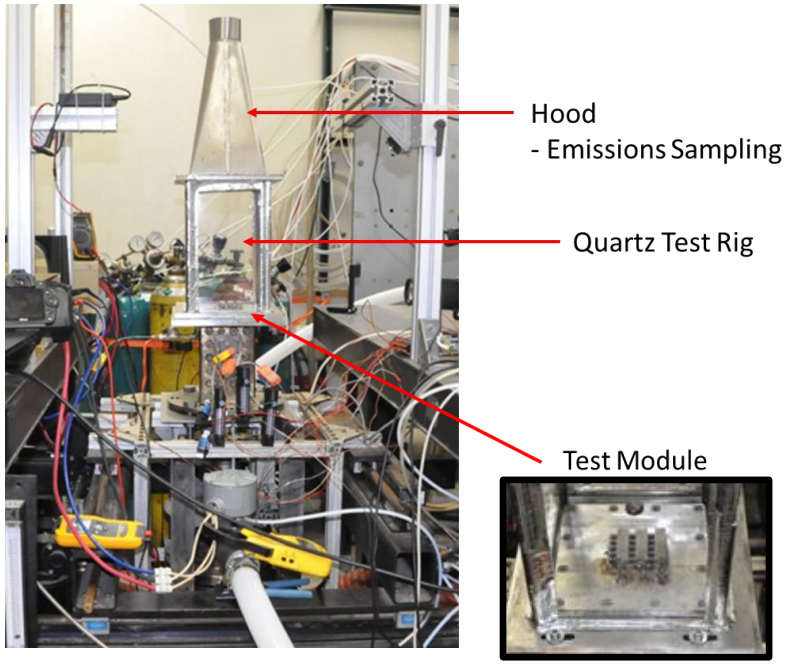

Low-pressure test rig at
Energy Research Consultants (ERC)

Solar Turbines - High H2 combustion data

- Flame diagnostic data using
  - High speed camera
  - OH chemiluminescence imaging
  - Schlieren imaging

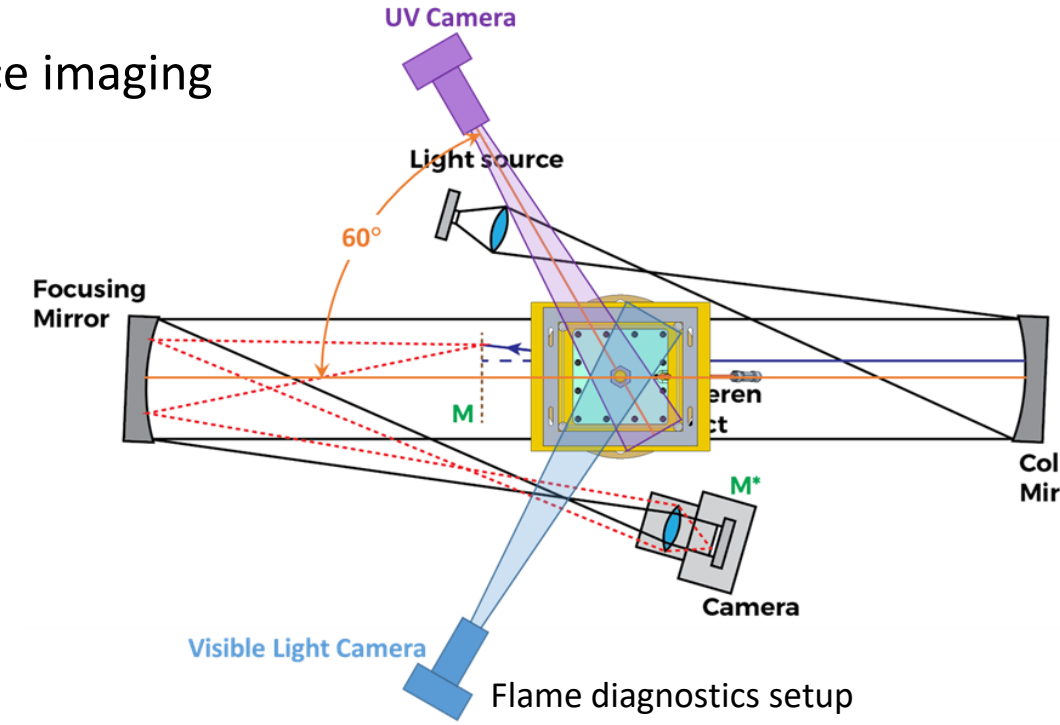

Flame diagnostics setup

Visible- High Speed Camera

OH image

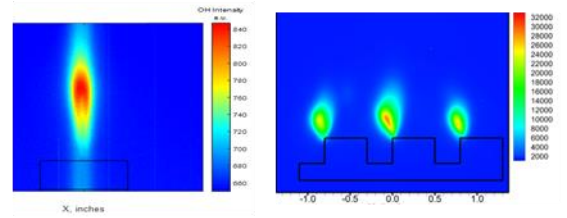

Schlieren image

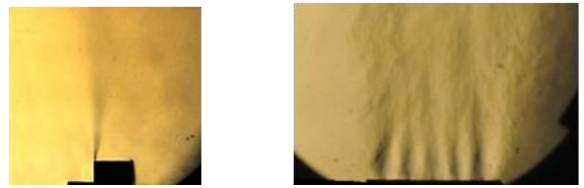

Flame data from ERC
(Left: single flame
Right: multi flames)

- CFD computation for design guideline

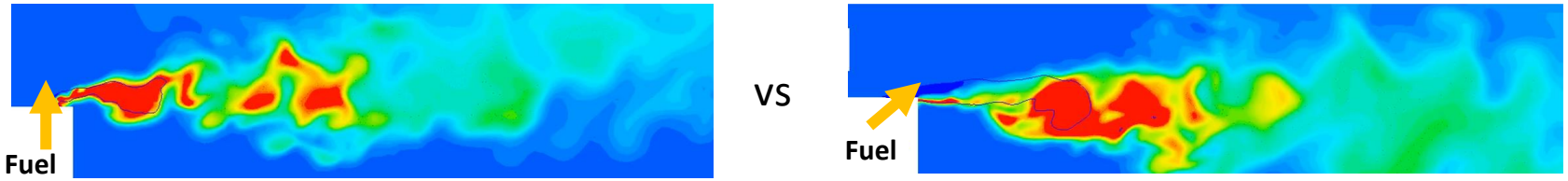

(Example: impact of injection angle)

Reacting Simulations

- $153 m/s$ H_2 jet in $150 m/s$ air co-flow
- Initial condition premixed at equivalence ratio of 0.5 at equilibrium

- Detailed chemistry with 8 species and 24 reactions
  - Based on the UCSD combustion mechanism of Williams et al. restricted to hydrogen-air combustion

- Molecular transport
  - Differential diffusion
    - Different species have different diffusion coefficients
  - Mixture-averaged formulation
    - As opposed to multicomponent, the diffusion coefficients are functions of the local concentrations only, not the concentration gradients
  - Soret and Dufour effects are neglected
    - They affect the laminar flame speed by 5% or less, hence are not expected to be significant here

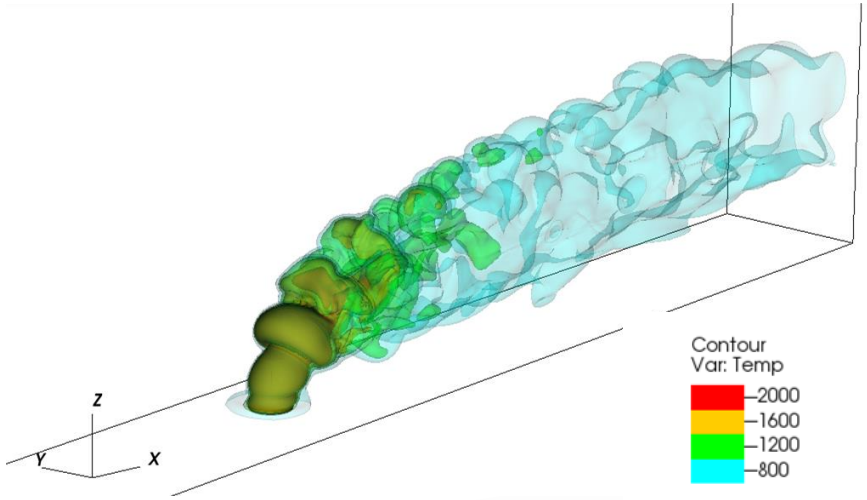

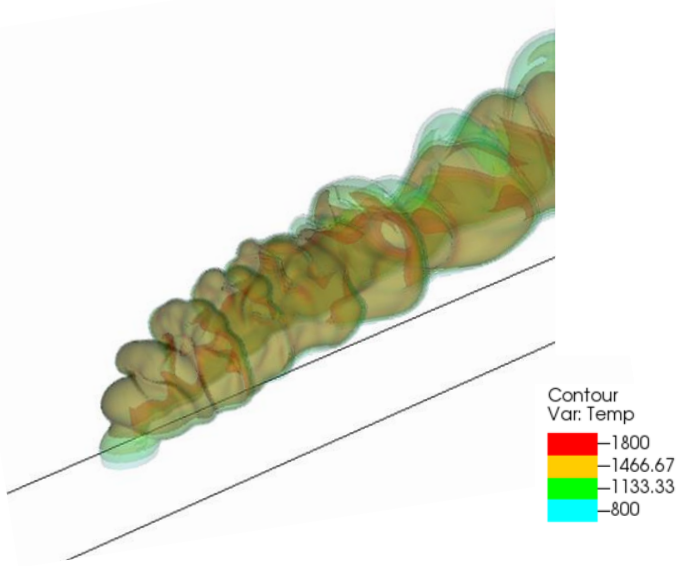

Baseline

Initial Conditions

- Blasius Profile in Cross-Stream
- Parabolic Profile in Injector
- Operating pressure : $P_a = 53,149\ Pa$

Boundary conditions

- Inlet: velocity type
  - ❑ Cross-stream inlet with Blasius BL
    - Blasius profile ($\delta = 3D$)
    - $T = 463\ K$
    - $Ma = 0.3 => u = 130[\frac{m}{s}]$
  - ❑ Jet inlet
    - ❑ Fully Developed Flow
    - $Re_D = 1000$
    - $v_j = 130\ [\frac{m}{s}] \quad (J = \frac{\rho_{cf} u_{cf}^2}{\rho_j u_j^2} = 1)$
    - $T = 463\ K$
- Outlet: pressure type
  - ❑ Damping Layer
    - Dampens to turbulent boundary specified by power law ($\delta = 5.62D$)

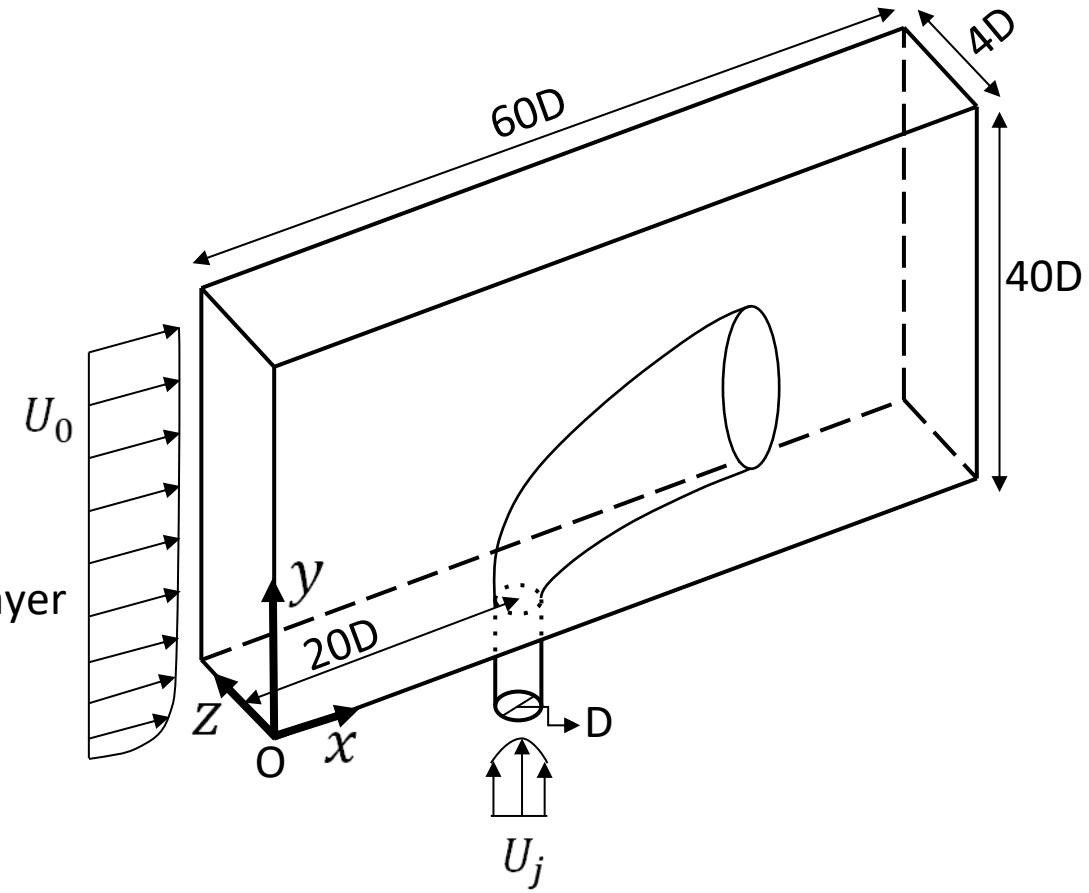

Solar Turbines - High H2 Combustion Data

Focus on injection region to establish design rules

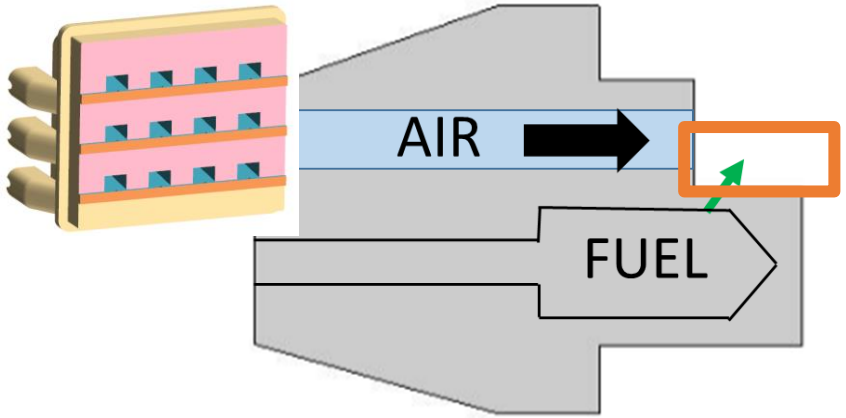

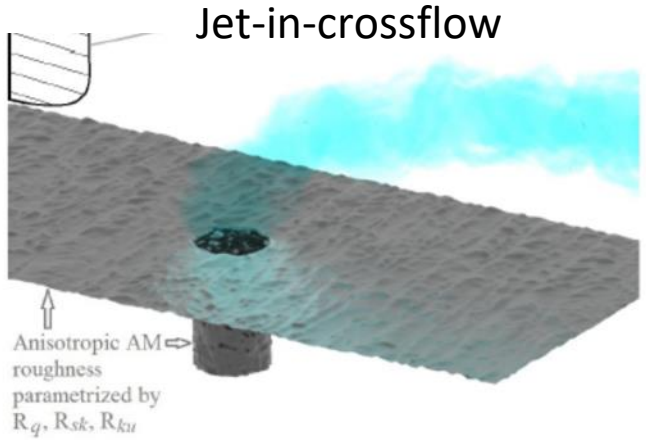

Using two code validation approach, parametrically investigate effects on flow physics and quantities of interest

Cold Flow:

- ✓ Validation
- ✓ Injector Spacing
- ❖ Injection Angle
- ➢ Inflow Conditions
  - ➢ Laminar/Turbulent
  - ➢ Turbulence Levels

Species Transport

- ✓ Injector Spacing

Reacting Flow

- ➢ Temperature Effets:
  - ➢ T_{H2}
  - ➢ T_{wall}

Solar Turbines – Update on Flow Conditions

- New developments suggest that a higher momentum ratio (injector to cross-stream) is potentially of interest
- In consult with Solar Turbines we are studying a higher J and compare it to lower J

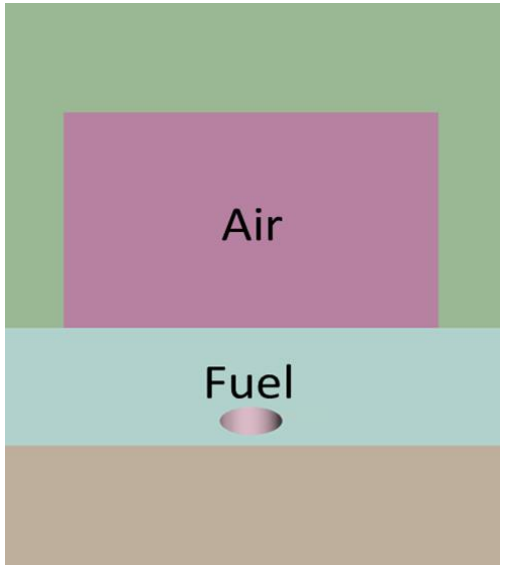

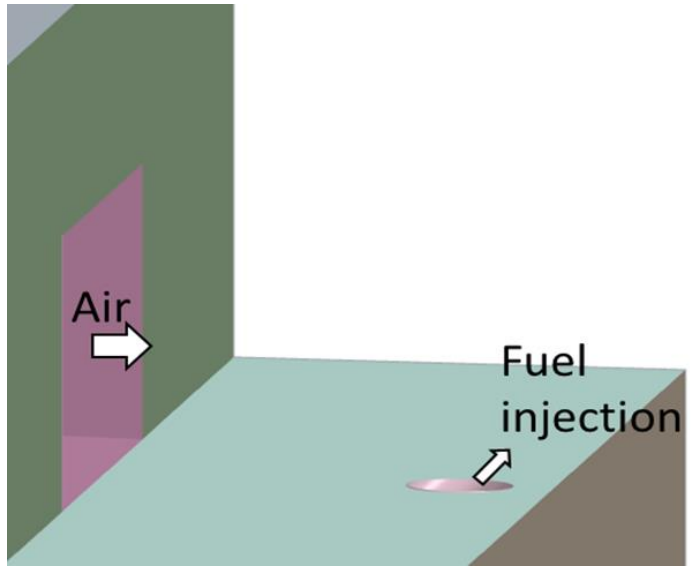

Fuel and Temperature Fields

- Hydrogen jet achieves significantly higher penetration, due to increased momentum ratio
- Flame is stabilized downstream from the jet
- Temperature is higher than for higher J, due to increased equivalence ratio

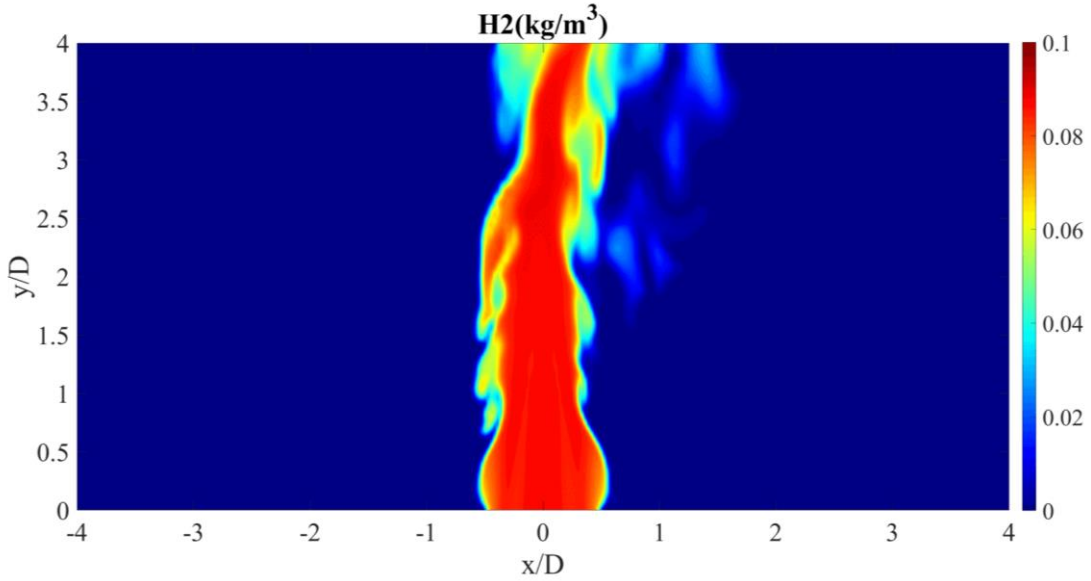

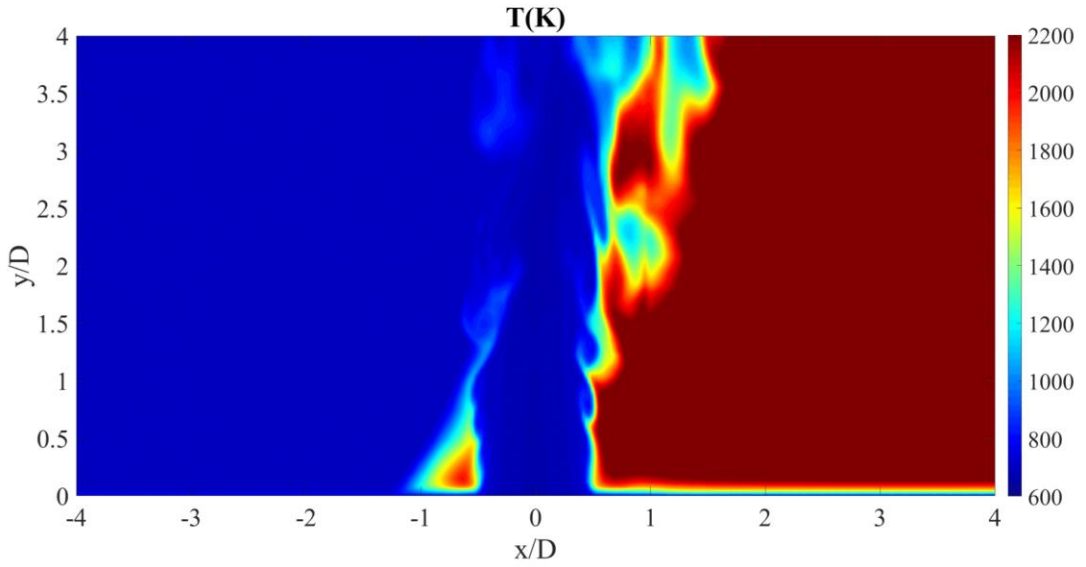

Velocity Fields

Horizontal velocity field is dominated by the Kelvin-Helmholtz fluctuations

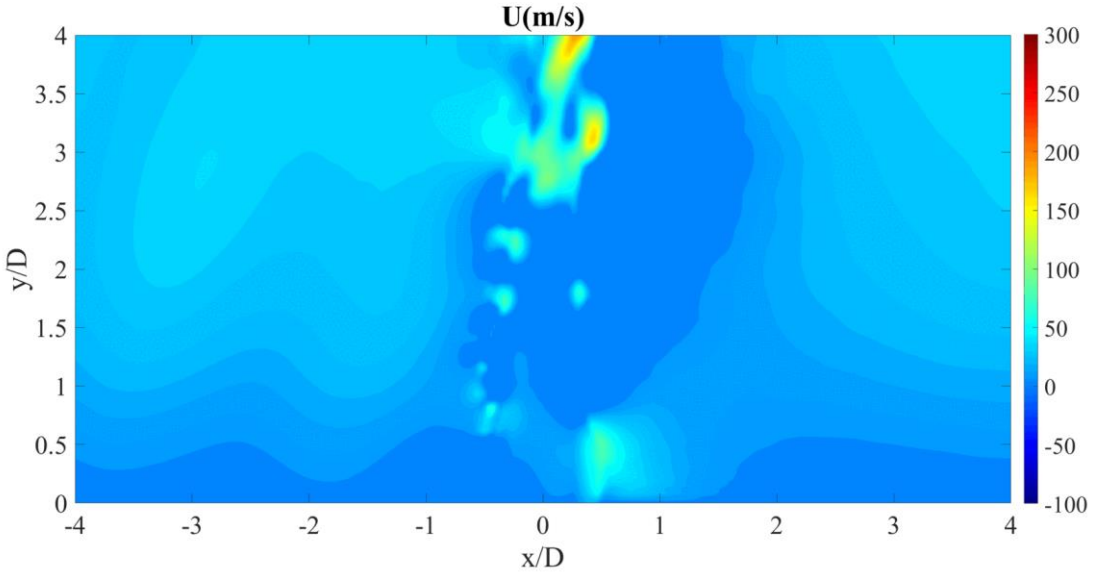

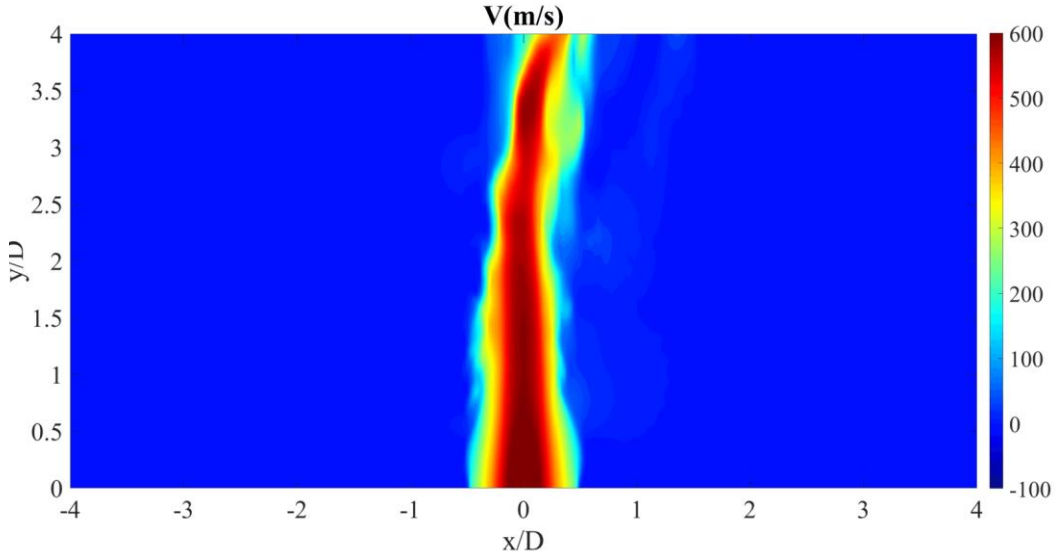

Radicals and Mixture Fraction Contours

- Region of high HO2 partial density corresponds to the region of heat release
- Here, the reaction region is situated one diameter above the burner wall

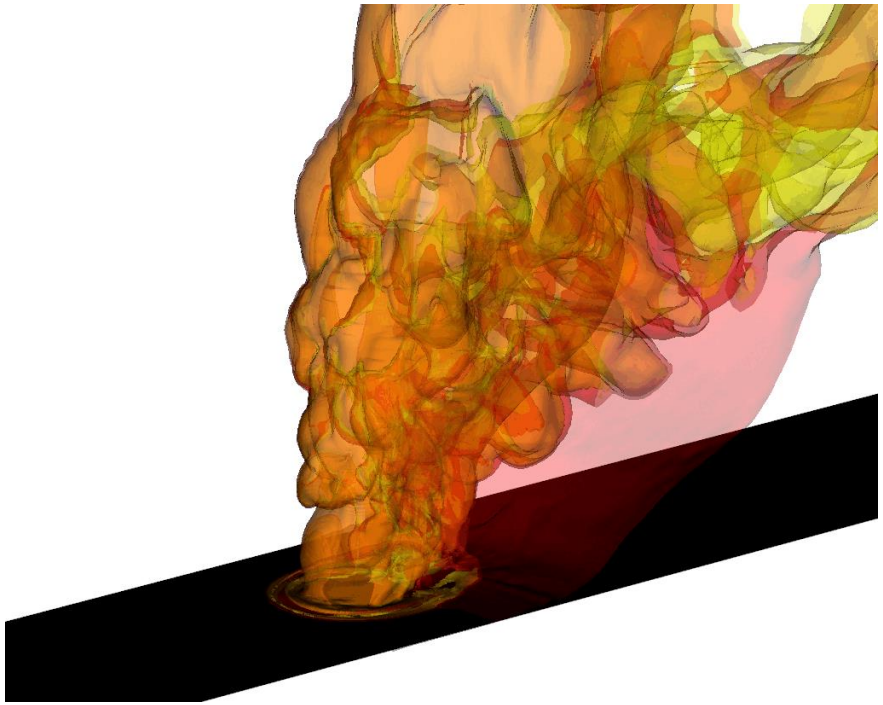

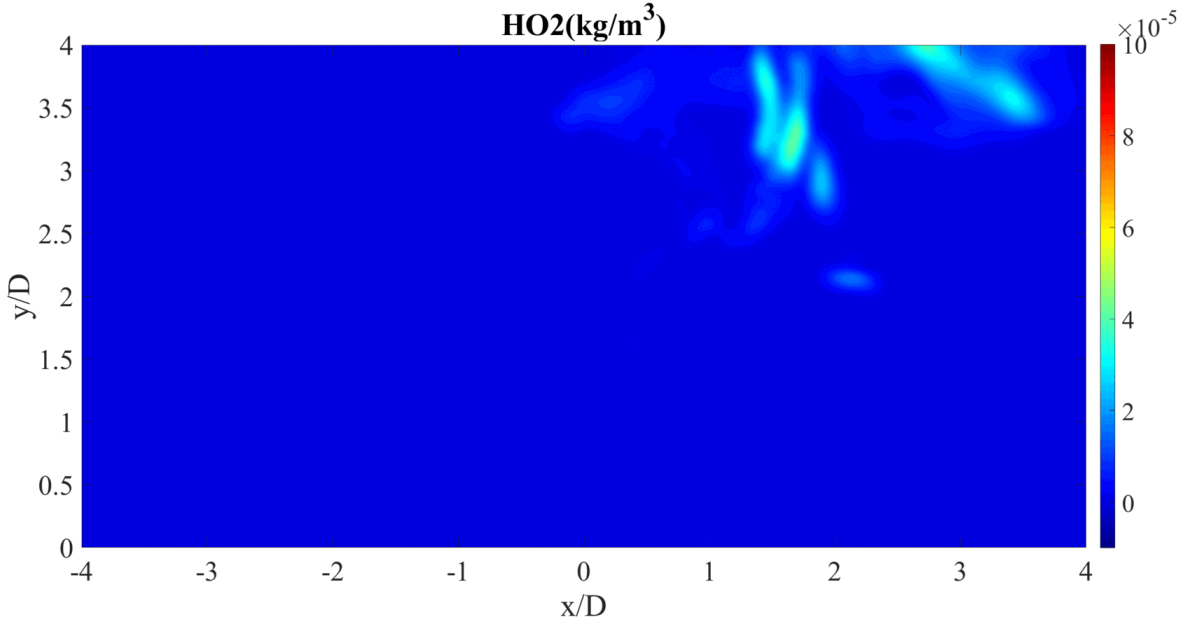

Mean Velocity and Temperature

- Normalized mean velocity is less monotonous than in the $130 m/s$ coflow case
- Effects of Kelvin-Helmholtz instability of the jet are more pronounced
- Maximum of mean temperature profile is similar between low- and high-momentum ratio case
- However, overall area under temperature profile is higher for the new high momentum ratio case
- Reason: large flow of hydrogen - equivalence ratio is closer to 1 in the high momentum ratio case – increased recirculation leads to transport of high-temperature fluid to the wall

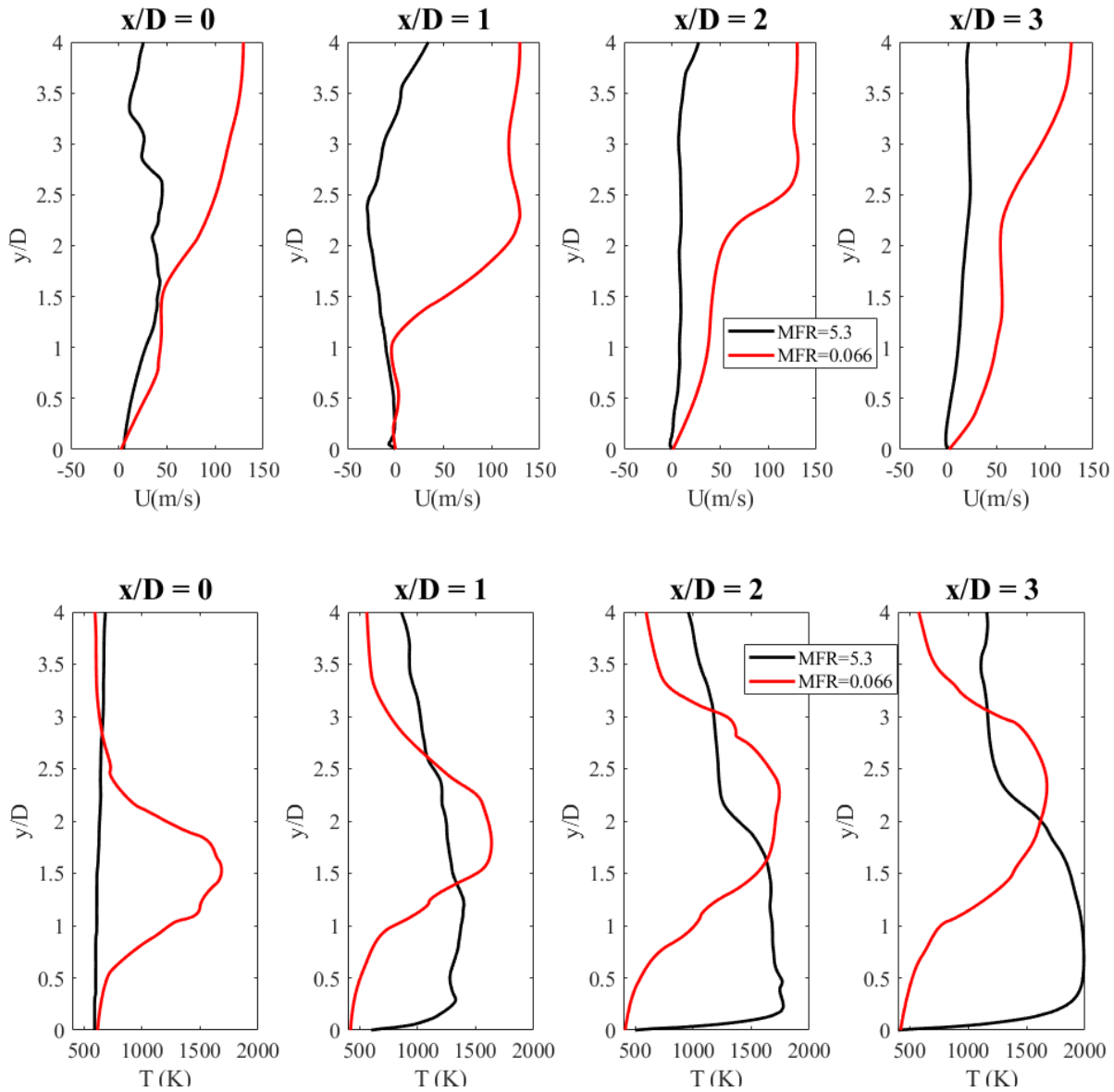

Combustion Product

- Mean HO2 partial density plots indicate flame region is above the high-temperature recirculation zone

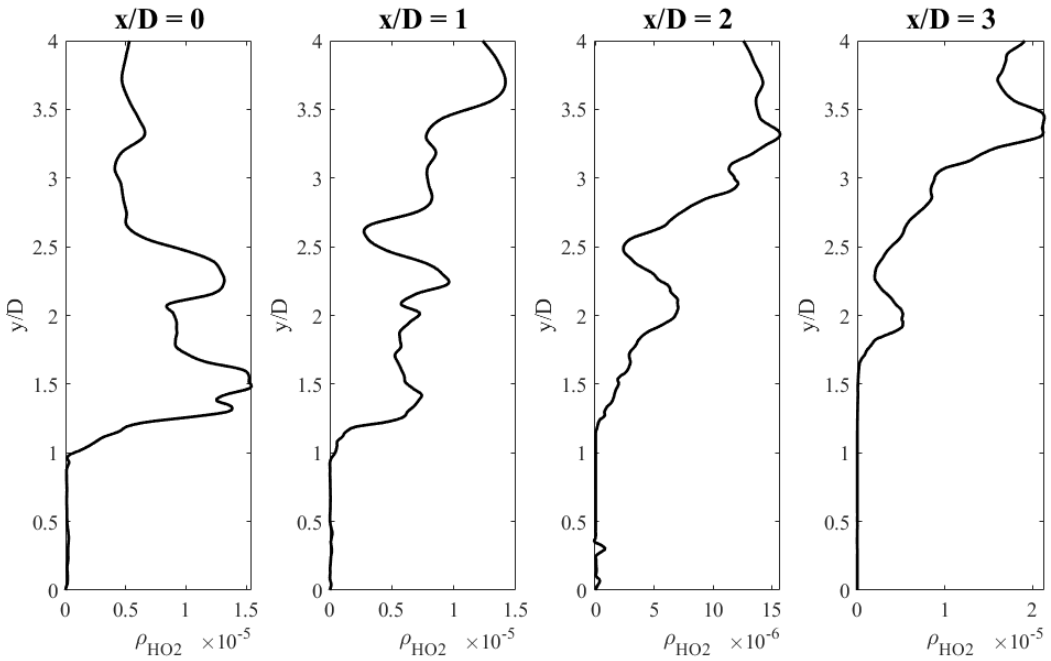

Machine Learning for Design Rules

$$T_{max} = T(x_{T_{max}})$$
$$\int_{CS}^{a} \mathbf{J_{H_2}} \cdot \mathbf{n}\, dS$$

Design Objective Function

$$\chi = 2D_t(\nabla Z \cdot \nabla Z)$$
$$U_{BO} = \frac{\left(\frac{\tau_c}{\tau_e}\right)^2 S_L^2 L}{\nu}$$

Intermediate QoIs

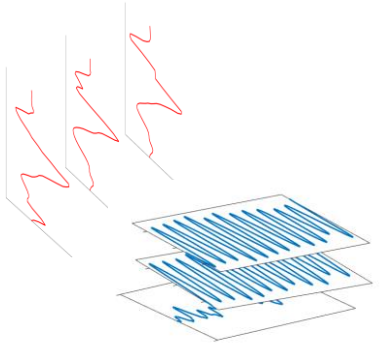

High-Fidelity Flow Data

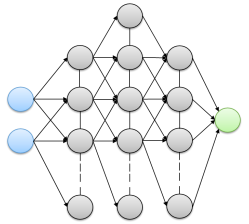

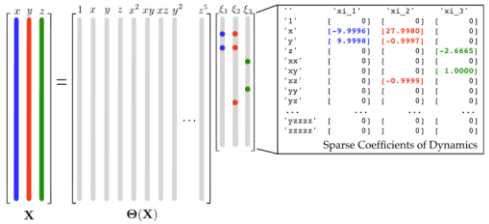

Machine learning

Surrogate and Dynamics Models

Optimal design

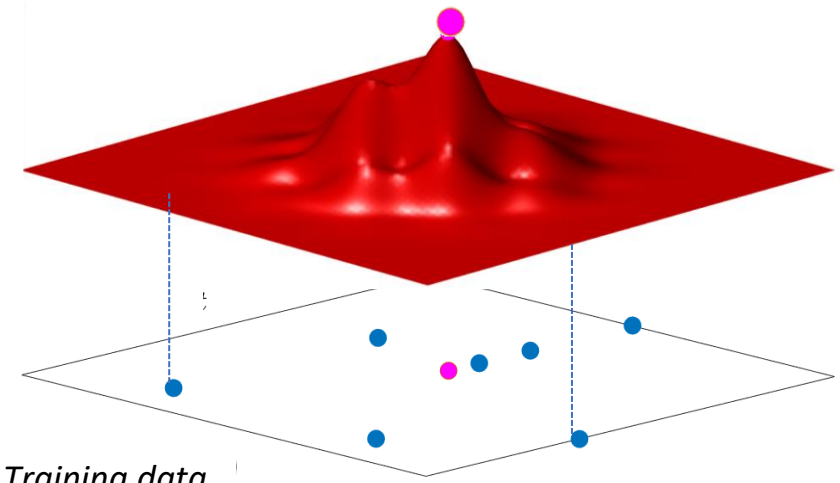

Training data

Reduced Dynamic Modeling SINDy

- Approximate flow dynamics from data

$$\frac{d}{dt}\boldsymbol{x}(t) = \boldsymbol{f}(\boldsymbol{x}(t))$$

where $\boldsymbol{x}(t)$ is the state variable (often POD modes)

- SINDy approximates the unknown $\boldsymbol{f}(\boldsymbol{x}(t))$ via the system

$$\boldsymbol{f}(\boldsymbol{x}(t)) = \Xi^T \Theta(\boldsymbol{x}^T)^T$$

where

  - $\Theta(\boldsymbol{x})$ is polynomial
  - SINDy solves for Ξ

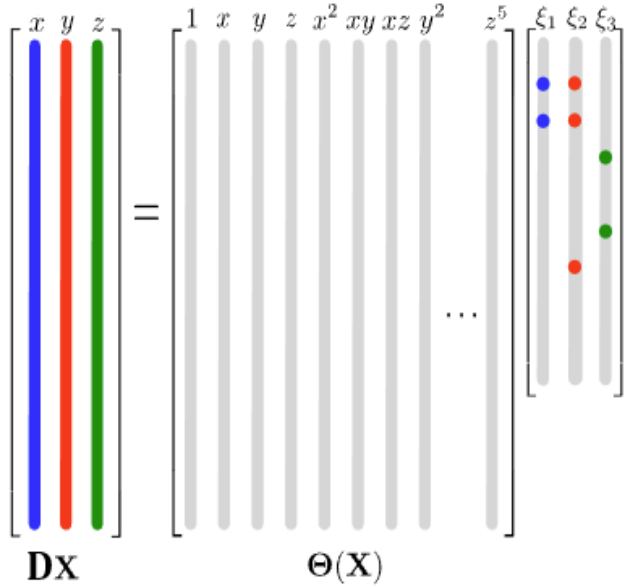

- Sparsity
  - sparsity parameter (λ) – determines the cutoff for setting entries of Ξ to 0
  - depends on degree of polynomial (P^0)

The reduced system is computationally efficient and can be used to determine statistics or identify new unsteady design limitation

[Brunton, Proctor, and Kutz, Proc. National Academy, 2016]

Proper Orthogonal Decomposition (POD)

POD find the orthogonal decomposition of a field

$$\mathbf{C}^{k\times k} = \frac{\mathbf{S}^T\mathbf{S}}{k} \rightarrow \mathbf{C}^{k\times k} = \mathbf{U}\Sigma V^T \rightarrow \mathbf{\Phi}^{m\times l} = \mathbf{S}\mathbf{U}^{k\times l} \rightarrow \boldsymbol{a}^{k\times l} = \mathbf{S}^{\mathrm{T}}\mathbf{\Phi}$$

$$\mathbf{S}^{m\times k} = \sum_{i=1}^{l} \phi_i a_i$$

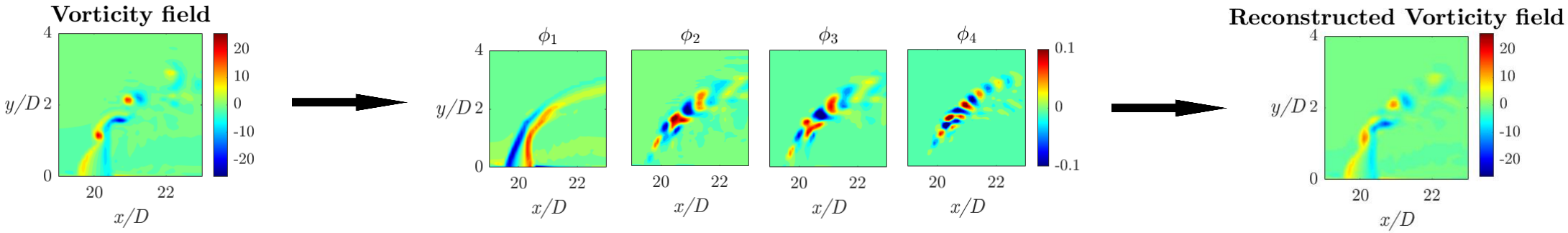

The first few POD modes are sufficient to calculate mean vorticity profiles

Training and Propagation

Propagation of a_n is bounded, exhibits consistent periodicity, and can be done for an extra 20 time units beyond the training time interval

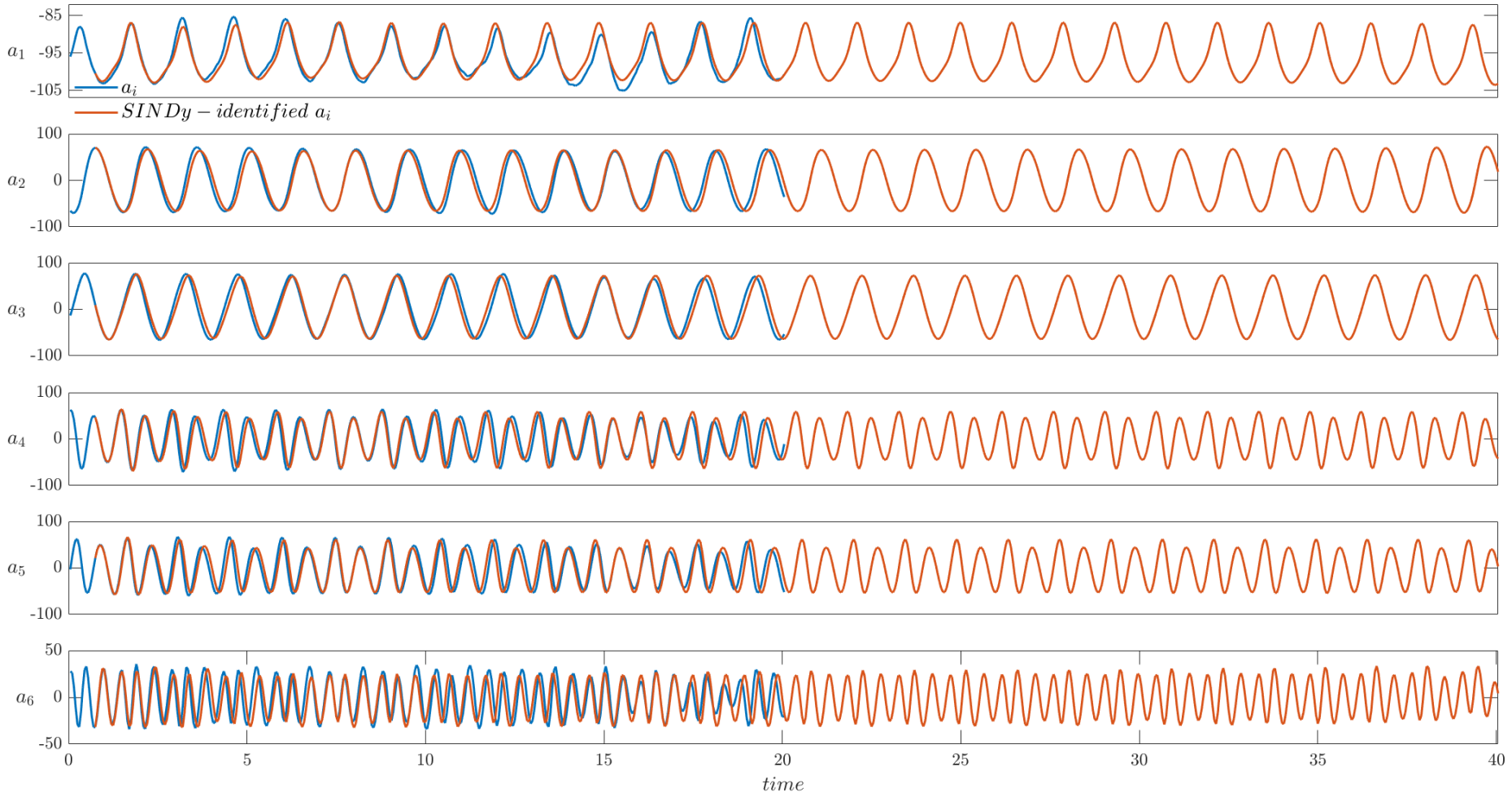

Vorticity Fields

- With increasing number of POD modes the approximation of the vorticity field improves
- Unsteady fields can be used to determine statistics and identifying time-dependent variables of interest to micro-mix designs

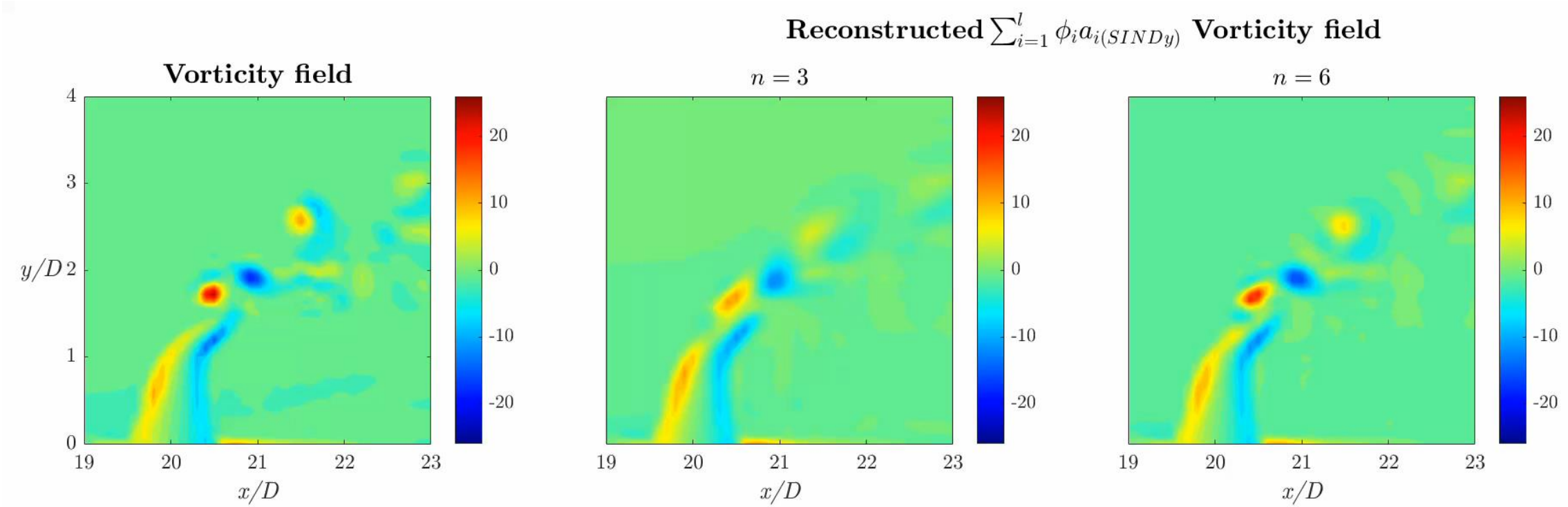

Mean Statistics with SINDy

- For mean statistics, $n = 3$ is sufficient
- Mean vorticity field approximation accuracy increases with n

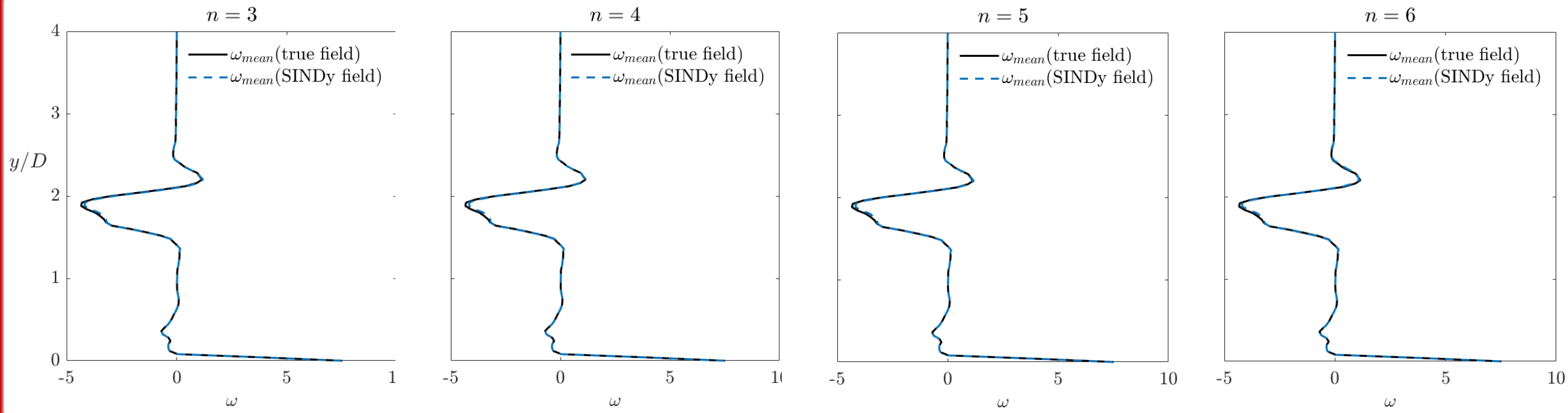

RMSE				
	$n = 3$	$n = 4$	$n = 5$	$n = 6$
$\boldsymbol{\omega_{mean}(SINDy)}$	2.95×10^{-2}	2.85×10^{-2}	2.82×10^{-2}	2.83×10^{-2}

Illustration ML: Optimal Injector Spacing

To illustrate development of design rules with reduced models

- determine the “optimal” injector spacing, l_{sp}
- adopt the perspective of dissipation of fuel mass fraction

Scalar dissipation rate of fuel mixture fraction, $\bar{\chi}$,is and indicator of fuel-air mixing levels

$$\bar{\chi} = \bar{\rho} D \widetilde{\nabla Z \cdot \nabla Z} \text{ can be closed as } \bar{\chi} = 2\bar{\rho} D_t (\widetilde{\nabla Z} \cdot \widetilde{\nabla Z})$$

$$\chi \propto \varepsilon \rightarrow \varepsilon = \mu \frac{\partial u_i}{\partial x_j} \frac{\partial u_i}{\partial x_j}$$

and is proportional to maximum vorticity

$$\omega \propto \frac{\partial u_i}{\partial x_j} \rightarrow \chi \propto \varepsilon \propto \omega^2$$

Let's find the maximum vorticity magnitude field for various injector spacings

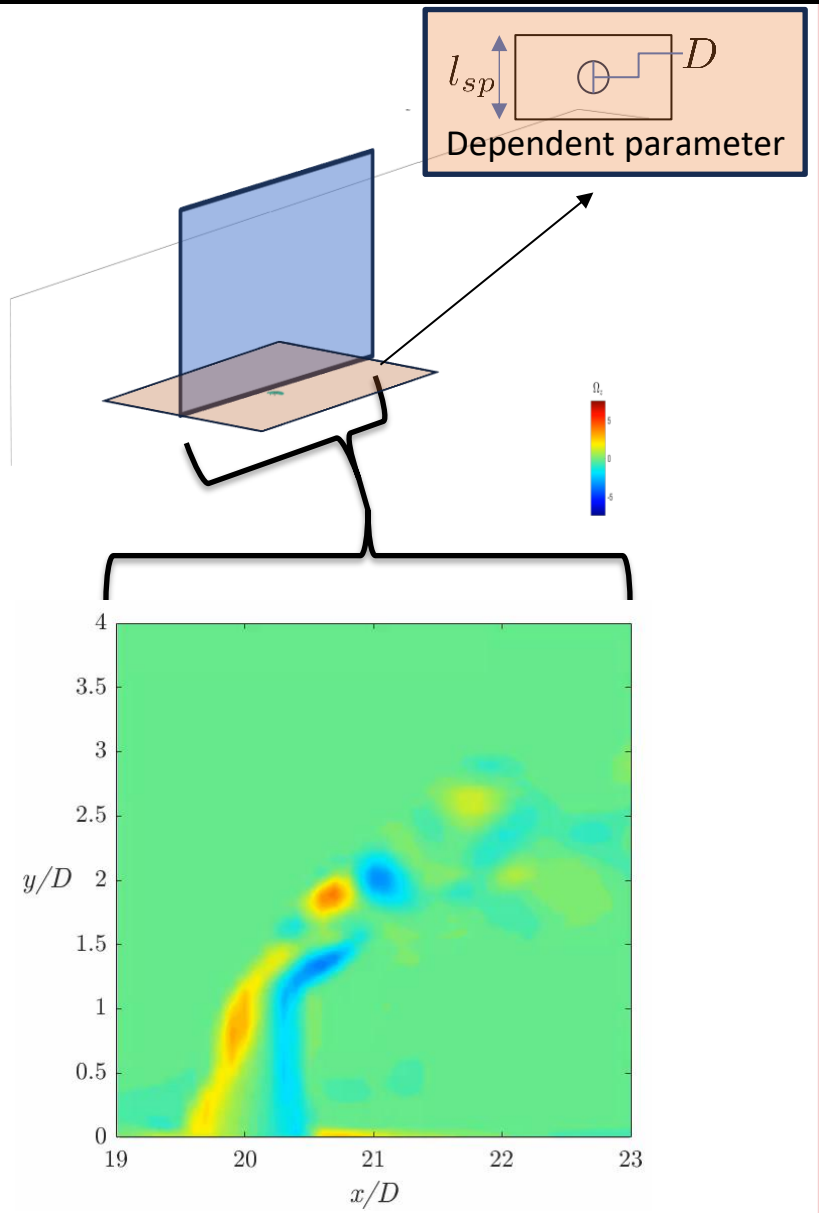

Step 1: Extract Maximum Vorticity with SINDy

SINDy can be used to find the maximum vorticity in a time accurate field in a computationally efficient manner

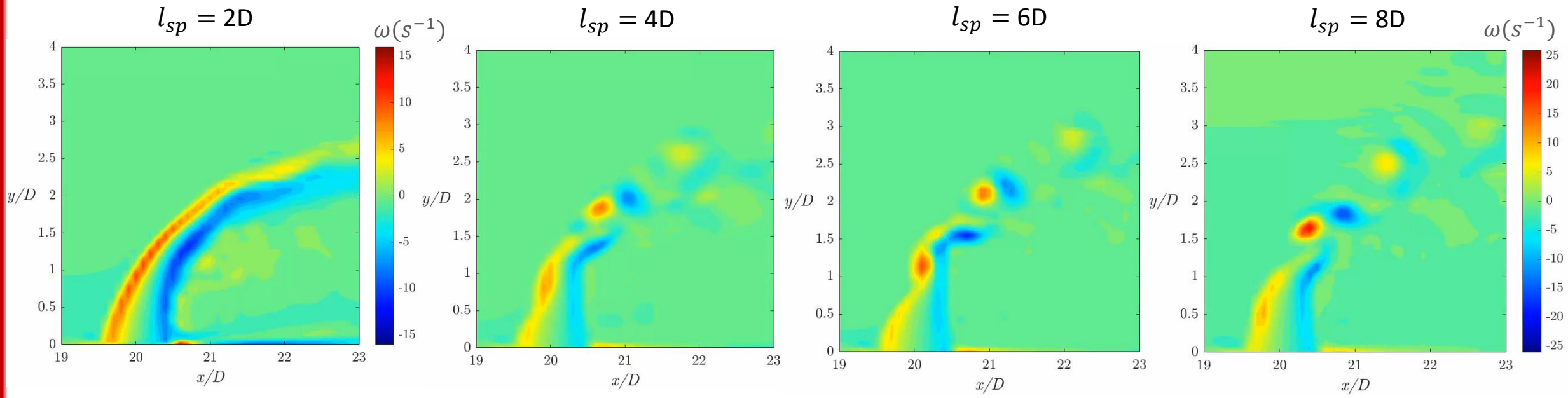

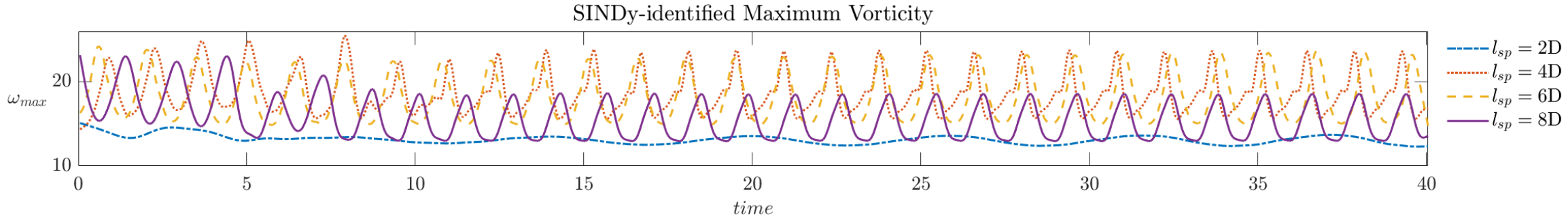

Step 2: Identify Optimal Design

$(\omega_{max}(t))^{max}_{l_{sp}=2D}$
$(\omega_{max}(t))^{max}_{l_{sp}=4D}$
$(\omega_{max}(t))^{max}_{l_{sp}=6D}$
$(\omega_{max}(t))^{max}_{l_{sp}=8D}$

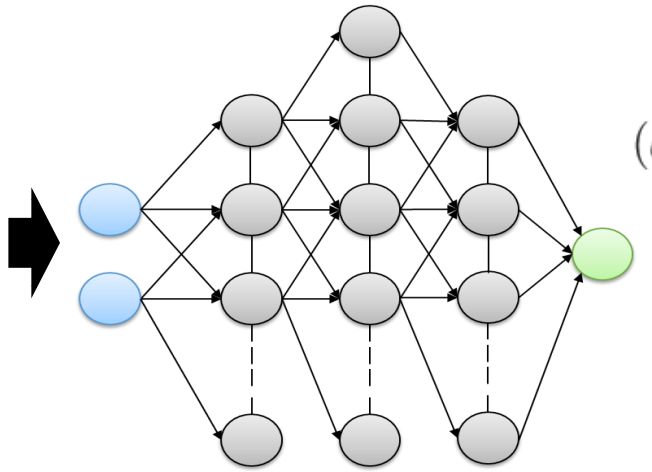

$(\omega_{max})^{max}$

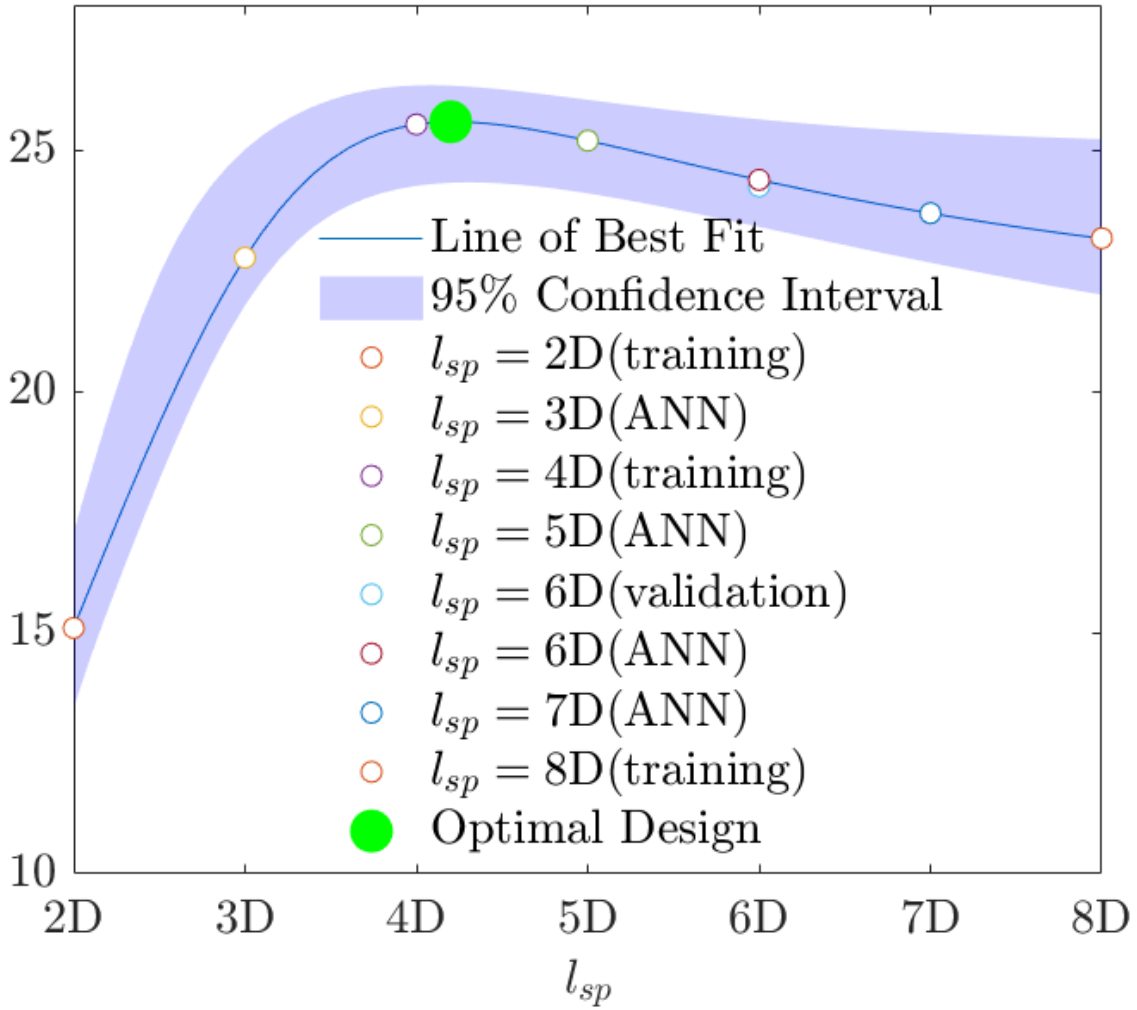

- Optimal design for maximizing χ : $l_{sp} = 4.2\text{D}$

Conclusions and Next Steps

Conclusions

- Wall roughness is implemented in the CFD solver
- The study on effect of flow conditions on the reacting H2 JICF has been expanded
- A framework that develops design rules for micro-mixers has been developed

Next Steps

- Expand the data base of high-fidelity simulations for chemically reacting flow
- Study the effect of wall roughness on chemically reacting flow
- Develop machine learned design rules